Molecular Neurobiology (2019) 56:2922–2943
https://doi.org/10.1007/s12035-018-1231-5

Biliverdin Reductase-A Mediates the Beneficial Effects of Intranasal Insulin in Alzheimer Disease

Eugenio Barone[1,2] · Antonella Tramutola[1] · Francesca Triani[1] · Silvio Calcagnini[3] · Fabio Di Domenico[1] · Cristian Ripoli[4,5] · Silvana Gaetani[3] · Claudio Grassi[4,5] · D Allan Butterfield[6] · Tommaso Cassano[7] · Marzia Perluigi[1]

Received: 1 May 2018 / Accepted: 10 July 2018 / Published online: 2 August 2018

Abstract

Impairment of biliverdin reductase-A (BVR-A) is an early event leading to brain insulin resistance in AD. Intranasal insulin (INI) administration is under evaluation as a strategy to alleviate brain insulin resistance; however, the molecular mechanisms underlying INI beneficial effects are still unclear. We show that INI improves insulin signaling activation in the hippocampus and cortex of adult and aged 3×Tg-AD mice by ameliorating BVR-A activation. These changes were associated with a reduction of nitrosative stress, Tau phosphorylation, and Aβ oligomers in brain, along with improved cognitive functions. The role of BVR-A was strengthened by showing that cells lacking BVR-A: (i) develop insulin resistance if treated with insulin and (ii) can be recovered from insulin resistance only if treated with a BVR-A-mimetic peptide. These novel findings shed light on the mechanisms underlying INI treatment effects and suggest BVR-A as potential therapeutic target to prevent brain insulin resistance in AD.

Keywords Alzheimer disease · Biliverdin reductase-A · Insulin resistance · Intranasal · Neuroprotection

Introduction

As populations age, the chronic diseases of older adults become increasingly important, not least to health systems and economies. Alzheimer disease (AD) has no proven preventative or behavioral intervention, and the currently approved pharmacological treatments are only modestly effective. The failure of insulin signaling, known as brain insulin resistance, heavily impacts the core pathological processes of AD since insulin regulates brain metabolism, cognitive functions, and life span [1, 2]. Examination of postmortem AD and amnestic mild cognitive impairment brain uncovered key signs of brain insulin resistance, i.e., reduced insulin receptor (IR) and increased serine phosphorylation (inhibitory) of insulin receptor substrate 1 (IRS1), particularly in the hippocampus, cortex, and hypothalamus [1–3]. Higher levels of insulin resistance markers are associated with poorer performance on cognitive tests of episodic and working memory, independent of the senile plaques and tangles load, thus suggesting a role for insulin signaling in neuronal functions [2].

Electronic supplementary material The online version of this article (https://doi.org/10.1007/s12035-018-1231-5) contains supplementary material, which is available to authorized users.

✉ Tommaso Cassano
tommaso.cassano@unifg.it

✉ Marzia Perluigi
marzia.perluigi@uniroma1.it

[1] Department of Biochemical Sciences "A. Rossi-Fanelli", Sapienza University of Rome, Piazzale A. Moro 5, 00185 Rome, Italy

[2] Instituto de Ciencias Biomédicas, Facultad de Salud, Universidad Autónoma de Chile, Avenida Pedro de Valdivia 425, Providencia, Santiago, Chile

[3] Department of Physiology and Pharmacology "V. Erspamer", Sapienza University of Rome, Piazzale A. Moro 5, 00185 Rome, Italy

[4] Institute of Human Physiology, Università Cattolica del Sacro Cuore, 00168 Rome, Italy

[5] Fondazione Policlinico Universitario A. Gemelli IRCCS, 00168 Rome, Italy

[6] Department of Chemistry, Markey Cancer Center, and Sanders-Brown Center on Aging, University of Kentucky, Lexington, KY 40506-0055, USA

[7] Department of Clinical and Experimental Medicine, University of Foggia, Via L. Pinto, 71122 Foggia, Italy

Insulin signaling contains several regulatory points, which represent critical nodes [4]. Among them, the protein biliverdin reductase-A (BVR-A) has emerged due to its pleiotropic functions. BVR-A—mainly known for its canonical activity in the degradation pathway of heme—is also a unique serine/threonine/tyrosine (Ser/Thr/Tyr) kinase directly involved in the regulation of insulin signaling at different levels [5, 6]. Previous studies identified several molecular features of BVR-A by showing that BVR-A is a direct target of the IR kinase activity, similar to IRS1. IR phosphorylates BVR-A on specific Tyr residues (Tyr198/228/291), resulting in activation of BVR-A kinase activity [5]. In turn, once activated by IR, BVR-A is able to phosphorylate IRS1 on Ser residues critical for the insulin signaling activation [5]. In addition, following insulin stimulation BVR-A is required for the activation and nuclear translocation of the extracellular signal-regulated kinases 1/2 (ERK1/2) [7] as well as for the correct activation of the protein kinase B (PKB/Akt) [8] known to regulate memory processes in the brain [9].

We demonstrated a significant impairment of BVR-A in human postmortem AD hippocampus [10, 11], and recent studies from our group also showed that the dysfunction of BVR-A is one of the earliest events characterizing the development of brain insulin resistance in AD [12]. Indeed, in a longitudinal study conducted with a triple-transgenic murine model of AD (3×Tg-AD), we identified three phases along the progression of AD pathology characterized by (1) reduced BVR-A protein levels associated with the hyper-activation of IR at 3 months of age, (2) reduced BVR-A levels and activation along with hyper-activation of both IR and IRS1 at 6 months of age, and (3) reduced BVR-A levels and activation associated with the activation of negative feedback pathways, e.g., mTOR aimed to turn-off IRS1 hyper-activity and thus leading to brain insulin resistance [12]. Furthermore, in vitro experiments in neuronal cell lines highlighted that insulin resistance phenomenon was characterized by a consistent impairment of BVR-A [12], an observation that strengthens the role of this protein as a regulator of the insulin signaling cascade.

Among the strategies to ameliorate the activation of the insulin signaling in the brain, intranasal insulin (INI) administration is under evaluation in an active large trial in the field of AD. Intranasal administration represents an effective strategy that allows drugs to bypass the blood brain barrier and directly reach the brain, thereby avoiding side effects caused by systemic administration [13]. Several small-scale clinical trials showed that INI improved memory and attention in healthy participants [14], as well as in patients with mild cognitive impairment and AD [14–16]. Preclinical studies in different mouse models of aging or AD confirmed the cognitive improvement obtained by INI [17–21] and also showed the path by which insulin reaches the brain [19, 20, 22–24]. However, it is still under debate the mechanism(s) by which INI administration might improve learning and memory and whether the INI treatment stimulates or not cerebral insulin signaling leading to a recovery from brain insulin resistance [25].

Therefore, the aim of the present study was to investigate the role of BVR-A in the activation of the insulin signaling cascade in the brain of both adult (6 months of age) and aged (12 months of age) 3×Tg-AD mice following INI administration. We found that INI administration was effective in (1) preventing the early impairment of BVR-A in adult mice and (2) recovering BVR-A activation in aged mice. Changes of BVR-A were positively associated with the amelioration of the insulin signaling cascade in the brain along with an improvement of AD neuropathology, cognitive, and non-cognitive functions. We also set up an in vitro protocol through which we were able to demonstrate that the lack of BVR-A functions is detrimental for cells and drives them toward insulin resistance. Furthermore, we demonstrated that BVR-A is essential to allow insulin to recover cells from insulin resistance.

These results confirmed that the impairment of BVR-A is an early event along the development of brain insulin resistance and that BVR-A could become a therapeutic target to prevent/rescue the alterations of the insulin signaling cascade in AD.

Methods

Animals

Four- and 10-month-old 3×Tg-AD male mice ($n = 8–10$ per group/treatment) and their wild-type (WT) male littermates ($n = 8–10$ per group/treatment) were used in this study. The 3×Tg-AD mice harbor 3 mutant human genes (APP_{Swe}, $PS1_{M146V}$, and tau_{P301L}) and have been genetically engineered by LaFerla and colleagues at the Department of Neurobiology and Behaviour, University of California, Irvine [26–28]. Colonies of homozygous 3×Tg-AD and WT mice were established at the vivarium of Puglia and Basilicata Experimental Zooprophylactic Institute (Foggia, Italy). The 3×Tg-AD mice background strain is C57BL6/129SvJ hybrid and genotypes were confirmed by PCR on tail biopsies [26]. The housing conditions were controlled (temperature 22 °C, light from 07:00–19:00, humidity 50%–60%), and fresh food and water were freely available. Animals received intranasal insulin (Humulin®R, Ely-Lilly, Inadianapolis, IN, USA) administration every other day (2 UI total, 4 μL/nostril) or vehicle (saline) during 2 months. All the experiments were performed in strict compliance with the Italian National Laws (DL 116/92) and the European Communities Council Directives (86/609/EEC). All efforts were made to minimize the number of animals used in the study and their suffering.

Animals were sacrificed at the selected age and the hippocampus and frontal cortex were extracted, flash-frozen, and stored at −80 °C until total protein extraction and further analyses were performed.

Behavioral Test

We used a serial behavioral testing procedure that has been validated and compared with single testing procedures in our laboratory, and by other investigators [29–32].

The novel object recognition (NOR) test and the Morris water maze (MWM) test were used to explore the cognitive behaviors, whereas the tail suspension test (TST) and the Porsolt forced swim test (FST) for antidepressant/depression-like coping behaviors. The experimental procedures were administered to the animals in this sequence, starting with those considered to be least stressful. The minimum interval between two consecutives procedures was 2 days. All tests were performed between 8:00 a.m. and 3:00 p.m., in a dimly lit condition. On the day of testing, the mice were acclimated for about 60 min in the behavioral room before the procedures were initiated. The apparatus was cleaned with 70% alcohol and water after each run. The behaviors were recorded with infrared lighting-sensitive CCD cameras, stored, and analyzed as MPEG files. Experimental subjects were weighed every day during the entire period of the experiment.

Novel Object Recognition Test The object recognition task is based on the spontaneous tendency of rodents to explore a novel object longer than a familiar one. Each mouse was habituated to an empty Plexiglas arena (45 × 25 × 20 cm) for 3 consecutive days. On training session (T1) (day 4), mice were exposed for 5 min to two identical objects (A + A) placed at opposite ends of the arena; 30 min and 24 h later, the animals were subjected to a 5-min testing session where they were exposed to one object familiar (A) and to a novel object B (after 30 min) and object C (after 24 h). Exploration was considered as pointing the head toward an object at a distance of < 2.5 cm from the object, with its neck extended and vibrissae moving. Turning around, chewing, and sitting on the objects were not considered exploratory behaviors. The time of exploration was recorded, and an object recognition index (ORI) were calculated, such that ORI = (TN − TF) / (TN + TF), where TN and TF represent times of exploring the familiar and novel object, respectively [31, 32]. Mice that did not explore both objects during training were discarded from further analysis. Objects used in this task were carefully selected to prevent preference or phobic behaviors. To avoid olfactory cues, the objects were thoroughly cleaned with 70% ethanol and the sawdust was stirred after each trial.

Morris Water Maze The test was conducted in a circular tank of 1.2 m in diameter, locates in a room with several extra maze cues as previously described [31]. Briefly, mice were trained to swim to a 14-cm-diameter circular Plexiglas platform submerged 1.5 cm beneath the surface of the water and invisible to the mouse while swimming. The water temperature was kept at 25 °C throughout the duration of the testing. The platform was fixed in place, equidistant from the center of the tank and its walls. Mice were subjected to four training trials per day and were alternated among four random starting points for 5 consecutive days. Mice were allowed to find and escape onto the submerged platform. If the mice failed to find the platform within 60 s, they were manually guided to the platform and were allowed to remain on it for 10 s. After this, each mouse was placed into a holding cage under a warming lamp for 25 s until the start of the next trial. Retention of the spatial training (the probe trial) was assessed 1.5 and 24 h after the last training session and consisted of a 60-s trial without the platform. Mice were monitored by a camera mounted in the ceiling directly above the pool, and all trials were stored on videotape for subsequent analysis. The parameters measured during the probe trial included (1) initial latency to cross the platform location and (2) time spent in the target quadrant (Scuderi et al., Transl Psychiatry 2018). Performance was monitored using the EthoVision XT version 7 video tracking software system (Noldus Information Technology Inc., Leesburg, VA).

Forced Swim Test The FST examines the dynamics of transition from an active (swimming) to a passive (immobility) mode of coping in an inescapable water-filled pool. Enhancement of immobility normally ensues after exposure, a phenomenon argued to reflect learned behavioral despair [29–32] and prevented by antidepressant treatment. The FST was performed as previously described [29–32]. Briefly, mice were placed individually into Plexiglas cylindrical bins (20 cm diameter, 50 cm high) filled with water (25–27 °C water temperature) to a depth of 20 cm. This depth did not allow the tail and hindpaws to touch the floor of the bin. The mice were allowed to swim for 6 min. After recording, the mice were rescued using a plastic grid and caged near a heat source (lamp). The behavioral tracking system was calibrated so that a mouse was considered immobile when making only those movements necessary to keep its head above water. The total duration of activity was determined during the last 4 min.

Tail Suspension Test This procedure, which is also used to assess antidepressant-like activity, involved suspending the mouse by the tail from a lever in a white box (30 × 30 × 30 cm). The test has duration of 6 min and is calculated by the immobility time (sec) in the last 4 min of recording. These

experimental conditions were similar to those previously described [29–32]. Antidepressant treatment reduces the total time the mouse remains immobile [30].

Samples Preparation

Total protein extracts were prepared in RIPA buffer (pH 7.4) containing Tris-HCl (50 mM, pH 7.4), NaCl (150 mM), 1% NP-40, 0.25% sodium deoxycholate, EDTA (1 mM), 0.1% SDS, supplemented with proteases inhibitors [phenylmethylsulfonyl fluoride (PMSF, 1 mM), sodium fluoride (NaF, 1 mM), and sodium orthovanadate (Na_3VO_4, 1 mM)]. Before clarification, brain tissues were homogenized by 20 passes with a Wheaton tissue homogenizer. Both brain tissues homogenates and collected cells were clarified by centrifugation for 1 h at 16,000×*g*, 4 °C. The supernatant was then extracted to determine the total protein concentration by the Bradford assay (Pierce, Rockford, IL).

Whole-Cell LTP in Organotypic Hippocampal Slices

Hippocampal organotypic slice cultures were prepared from postnatal day 4–7 rats through a McIllwain tissue chopper as previously described in Spinelli et al. 2017. Slices (350 μm) were placed on semiporous membranes (Millipore) fed by tissue medium (for 1 l: 788 ml 1×MEM (GIBCO, No. 11575–032, 7.16 g HEPES, 0.49 g $NaHCO_3$, 4.8 g D-glucose, 50 μl 25% ascorbic acid, 50 μl (10 mg/ml) insulin, 200 ml horse serum, 2 ml 1 M $MgSO_4$, 1 ml 1 M $CaCl_2$). Slices were incubated at 35 °C in 5% CO_2 and after 5–7 days CA1 pyramidal neurons were transfected with ballistic gene transfer (Gene-Gun, Bio-Rad, CA, USA). shRNAs were transfected together with a plasmid enconding enhanced green fluorescent protein (EGFP) to identify the transfected neurons. LTP experiments were performed 2 days after transfection after stimulating the Schaffer collateral fibers by means of a bipolar tungsten electrode (FHC, Neural microTargeting Worldwide) as previously described [33, 34]. Slices were incubated in artificial cerebrospinal fluid (ACSF) containing (in mM): 119 NaCl, 2.5 KCl, 4 $CaCl_2$, 4 $MgCl_2$, 1 NaH_2PO_4, 26 $NaHCO_3$, 11 D-glucose, and 0.005 2-chloroadenosine, gassed with 95% O_2/5% CO_2. Whole-cell recording pipettes (3–4 MΩ) were filled with a solution containing (in mM) 135 $CsMeSO_3$, 8 NaCl, 10 HEPES, 0.25 EGTA, 2 Mg_2ATP, 0.3 Na_3GTP, 0.1 spermine, 7 phosphocreatine, and 5 QX-314, pH 7.25–7.30 (osmolarity 300). Data were collected with a MultiClamp 700B amplifier (Molecular Devices), digitized at 10 kHz using the Digidata 1440A data acquisition system (Molecular Devices) and analyzed using Clampfit software (Molecular Devices). LTP was induced by pairing 200 stimuli at 2 Hz with a holding potential of 0 mV. To avoid "wash-out" of LTP, the induction protocol was applied within 5–7 min of achieving whole-cell configuration. The magnitude of LTP was calculated on basis of the averaged EPSC values during the last 5 min of recordings (from min 25 to min 30). LTP magnitude was expressed as the percentage change in the mean EPSC peak amplitude normalized to baseline values 100% (i.e., mean values of recording before LTP induction).

Cell Culture and Treatments

The HEK cells were grown in Dulbecco's modified Eagle's medium (DMEM) supplemented with 10% fetal bovine serum (FBS), 2 mM L-glutamine, penicillin (20 units/ml), and streptomycin (20 mg/ml), (GIBCO, Gaithersburg, MD, U.S.A.). Cells were maintained at 37 °C in a saturated humidity atmosphere containing 95% air and 5% CO_2. Cells were seeded at density of $40 \times 10^3/cm^2$ in six-well culture dishes for the subsequent treatments aimed to (i) induce the activation the insulin signaling cascade, (ii) induce insulin resistance, and (iii) recovery cells from insulin resistance. These experiments have been performed based on a previous published protocol further modified for the scope of this paper. In a first set of experiments, HEK cells were treated with insulin (humulin®R, Ely-Lilly, Inadianapolis, IN, USA) 100 nM for different times (2–6–12–24 h) to select the best time-to-treatment to be used in the other experiments. Then, to mimic insulin overexposure known to promote insulin resistance [35], at the selected time, cells were treated with an additional dose of insulin (100 nM) for other 2 h. Thereafter, medium was discarded, cells were washed twice with PBS, and rechallenged with DMEM with 10% FBS containing insulin (100 nM–500 nM–1 μM) for additional 2 h to mimic the effect of INI treatment aimed to recover insulin signaling cascade activation. In parallel, to test the effects produced by the silencing of BVR-A on insulin signaling activation, HEK cells were seeded at density of $40 \times 10^3/cm^2$ in six-well culture dishes. After 24 h, medium has been replaced with DMEM with 10% FBS, without antibiotics. Following, cells have been transfected with 10 pmol of a small interfering RNA (siRNA) for BVR-A (Ambion, Life Technologies, LuBioScience GmbH, Lucerne, Switzerland, No. 4392420) using Lipofectamine® RNAiMAX reagent (Invitrogen, Life Technologies, LuBioScience GmbH, Lucerne, Switzerland, No. 13778-030) according to the manufacturer's protocol, and then treated with insulin as described above. At the end of each treatment, cells were washed twice with PBS, collected, and proteins were extracted as described below.

Peptide Treatments

HEK cells were plated as described above and then treated with the myristoilated peptide (myr-KYCCSRK) (Biomatik, Wilmington, Delaware, USA) at the dose of 10 and 20 μM [6, 36] in combination with insulin (100 or 500 nM) for 2 h.

Slot Blot Analysis

To evaluate total (i) protein-bound 4-hydroxy-2-nonenals (HNE) and (ii) 3-nitrotyrosine (3-NT) levels, brain samples (5 μl), 12% SDS (5 μl), and 5 μl modified Laemmli buffer containing 0.125 M Tris base, pH 6.8, 4% (*v*/*v*) SDS, and 20% (*v*/*v*) glycerol were incubated for 20 min at room temperature and then loaded onto nitrocellulose membrane as described below.

Proteins (250 ng) were loaded in each well on a nitrocellulose membrane under vacuum using a slot blot apparatus. The membrane was blocked in blocking buffer (3% bovine serum albumin) in PBS 0.01% (*w*/*v*) sodium azide and 0.2% (*v*/*v*) Tween 20 for 1 h and incubated with an anti-2,4-dinitrophenylhydrazone (DNP) adducts polyclonal antibody (1:100, EMD Millipore, Billerica, MA, USA, No. MAB2223) or HNE polyclonal antibody (1:2000, Novus Biologicals, Abingdon, UK, No. NB100-63093) or an anti 3-NT polyclonal antibody (1:1000, Santa Cruz, Santa Cruz, CA, USA, No. sc-32757) in PBS containing 0.01% (*w*/*v*) sodium azide and 0.2% (*v*/*v*) Tween 20 for 90 min. The membrane was washed in PBS following primary antibody incubation three times at intervals of 5 min each. The membrane was incubated after washing with an anti-rabbit IgG alkaline phosphatase secondary antibody (1:5000, Sigma-Aldrich, St. Louis, MO, USA) for 1 h. The membrane was washed three times in PBS for 5 min each and developed with Sigma fast tablets (5-bromo-4-chloro-3-indolyl phosphate/nitroblue tetrazolium substrate [BCIP/NBT substrate]). Blots were dried, acquired with Chemi-Doc MP (Bio-Rad, Hercules, CA, USA), and analyzed using Image Lab software (Bio-Rad, Hercules, CA, USA). No non-specific binding of antibody to the membrane was observed.

Western Blot

For western blots, 30 μg of proteins were resolved on Criterion TGX Stain-Free 4–15% 18-well gel (Bio-Rad Laboratories, No. 5678084) in a Criterion large format electrophoresis cell (Bio-Rad Laboratories, No. 1656001) in TGS Running Buffer (Bio-Rad Laboratories, No. 1610772). Immediately after electrophoresis, the gel was then placed on a Chemi/UV/Stain-Free tray and then placed into a ChemiDoc MP imaging System (Bio-Rad Laboratories, No. 17001402) and UV-activated based on the appropriate settings with Image Lab Software (Bio-Rad Laboratories) to collect total protein load image. Following electrophoresis and gel imaging, the proteins were transferred via the TransBlot Turbo semi-dry blotting apparatus (Bio-Rad Laboratories, No. 1704150) onto nitrocellulose membranes (Bio-Rad, Hercules, CA, USA, No. 162-0115) and membranes were blocked with 3% bovine serum albumin in 0.5% Tween-20/Tris-buffered saline (TTBS) and incubated overnight at 4 °C with the following antibodies: anti-BVR-A (1:5000, abcam, Cambridge, UK, No. ab90491), anti-BVR-A (1:1000, Sigma-Aldrich, St Louis, MO, USA, No. B8437), anti-IRβ (1:1000, Cell Signaling, Bioconcept, Allschwill, Switzerland, No. 3020), anti-phospho(Tyr1158/1162/1163)-IRβ (1:1000, Genetex, Irvine, CA, USA, No. GTX25681), anti-IRS1 (1:1000, Cell Signaling, Bioconcept, Allschwill, Switzerland, No. 3407), anti-phospho(Ser307)-IRS1 (1:500, Cell Signaling, Bioconcept, Allschwill, Switzerland, No. 2381), anti-phospho(Ser636)-IRS1 (1:500, Santa Cruz, Santa Cruz, CA, USA, No. sc-33957), anti-Akt (1:1000, 1:1000, Bio-Rad Laboratories, No. vma00253k), anti-phospho(Ser473)-Akt (1:1000, Cell Signaling, Bioconcept, Allschwill, Switzerland, No. 193H12), anti-ERK1/2 (1:1000, Cell Signaling, Bioconcept, Allschwill, Switzerland, No. 9102), anti-phospho(Thr202/Tyr204)-ERK1/2 (1:1000, Cell Signaling, Bioconcept, Allschwill, Switzerland, No. 9101), anti-mTOR (1:1000, Bio-Rad Laboratories, No. vpa00174k), anti-phospho(Ser2448)-mTOR (1:500, Cell Signaling, Bioconcept, Allschwill, Switzerland, No. 5536), anti-phospho-Tyrosine (1:2000, Cell Signaling, Bioconcept, Allschwill, Switzerland, No. 9416), anti-IDE (1:1000, Santa Cruz Biotechnology, No. sc-393887), purified anti-Ab 1-16 (1:1000, 6E10, Signet Laboratories-Covance, Emeryville, CA, USA, No. SIG-39320), anti-Tau (1:1000, Santa Cruz, Santa Cruz, CA, USA, No. sc-5587), anti-phospho(Ser202, Thr205)-Tau (1:1000, AT8, Thermo Scientific, Waltham, MA, USA, No. MN1020). After three washes with TTBS, the membranes were incubated for 60 min at room temperature with anti-rabbit/mouse/goat IgG secondary antibody conjugated with horseradish peroxidase (1:5000; Sigma-Aldrich, St. Louis, MO, USA). Membranes were developed with Clarity ECL substrate (Bio-Rad Laboratories, No. 1705061) and then acquired with Chemi-Doc MP (Bio-Rad, Hercules, CA, USA) and analyzed using Image Lab software (Bio-Rad, Hercules, CA, USA) that permits the normalization of a specific protein signal with the β-actin signal in the same lane or total proteins load.

Immunoprecipitation

The immunoprecipitation procedure was performed as previously described [37], with minor modifications. Briefly, 150 μg of proteins were dissolved in 500 μL of RIPA buffer (10 mM Tris, pH 7.6; 140 mM NaCl; 0.5% NP-40) supplemented with proteases inhibitors and incubated with 1 μg anti-BVR-A polyclonal antibody at 4 °C overnight. Immunocomplexes were collected using protein A/G suspension for 2 h at 4 °C and washed five times with immunoprecipitation buffer. Immunoprecipitated BVR-A was recovered by re-suspending the pellets in reducing sodium dodecyl sulfate buffers and electrophoresing them on 12% gels, followed

by western blot analysis. Total BVR-A was used as a loading control as previously described [7, 10, 11, 38].

Statistical Analyses

All data are presented as means ± SEM of *n* independent samples per group. Behavioral and biochemical data were analyzed by two-way analyses of variance (ANOVA) with genotype (3×Tg-AD vs WT) and treatment (insulin vs vehicle) as between-subject factors. Tukey's honestly significant difference (HSD) test or Bonferroni's test were used for multiple post hoc comparisons when required. Student *t* test was used to evaluate differences observed in cellular experiments. $p < 0.05$ was considered significantly different from the reference value. All statistical analysis was performed using GraphPad Prism 5.0 software.

Results

Intranasal Insulin Administration Improves Short-Term Learning and Memory in 6- and 12-Month-Old 3×Tg-AD Mice

We tested the effects of insulin treatment on both short- and long-term memory in both 6- and 12-month-old 3×Tg-AD mice and age-matched WT littermates, performing hippocampal- and cortical-dependent tasks as measured by Morris water maze (MWM) and novel object recognition (NOR) tests. Statistical details are reported in Supplementary Table 1. After behavioral testing, mice were sacrificed and brain collected for further biochemical analysis (Fig. 1a).

Spatial learning and memory were measured by MWM, in which mice received four training trials/day for 5 consecutive days to locate the hidden platform. Statistics demonstrated no difference in spatial memory during 5 days of training (acquisition) among all experimental groups at 6 and 12 months of age, indicating there is no difference in motivation or ability to perform the task (Fig. 1b). To determine the effects of insulin on memory, the platform was removed from the maze, and tests were conducted 1.5 or 24 h following the last training trial to independently assess both short- and long-term memory, respectively. Insulin significantly rescued the short-term (1.5 h) spatial memory deficits present in both 6- and 12-month-old 3×Tg-AD mice, as indicated by a significantly decreased latency to cross the platform location and increased time spent in target quadrant of the 3×Tg-AD mice treated with insulin compared to vehicle-treated 3×Tg-AD (Fig. 1c, d). Moreover, insulin had no significant effects on learning or memory retention in WT mice. When a probe session was performed at 24 h (long-term memory) after the last training session, at 6 months of age, insulin induced only a trend toward a decrease (−32%) in the 3×Tg-AD compared to vehicle-treated 3×Tg-AD mice (Fig. 1c); conversely, the latency to cross platform location was significantly decreased (−58%) at 12 months of age in insulin-treated 3×Tg-AD mice compared to age-matched vehicle-treated 3×Tg-AD mice (Fig. 1c). Regarding the time spent in the target quadrant at 24 h after the last training session, insulin induced only a trend toward an increase in the 3×Tg-AD compared to vehicle-treated 3×Tg-AD mice (+ 35% and + 52%, respectively, at 6 and 12 months of age) (Fig. 1d). Finally, multiple post hoc comparisons showed that 3×Tg-AD mice treated with insulin performed similarly to the WT mice in all probe trials and at both time points.

The NOR test exploits the natural tendency of mice to explore objects perceived as novel. As previously described, the retention session was performed at two different time points (30 min or 24 h) after the exploration session in order to assess both short- and long-term memory, respectively. Two-way ANOVA for the object recognition index (ORI) at a time-point of 30 min (short-term memory) either in 6- and 12-month-old mice revealed a significant main effect of genotype and treatment, while no significant genotype-by-treatment interaction effect was found. Multiple post hoc comparisons showed a significant higher ORI in insulin-treated 3×Tg-AD with respect to vehicle-treated 3×Tg-AD mice, indicating that insulin significantly improves the short-term recognition memory in the 3×Tg-AD mice (Fig. 1e). When the probe trial was performed 24 h after the exploration session (long-term memory), we observed only a significant main effect of genotype among the four groups (Fig. 1e). Although insulin-treated 3×Tg-AD mice performed better than vehicle-treated 3×Tg-AD mice, multiple post hoc comparisons did not reach any significant difference (+ 26% and + 21%, respectively, at 6 and 12 months of age). Finally, at both time points, the post hoc analysis indicated that insulin had no effect on the performance of WT mice.

Overall, these data indicate that insulin significantly both prevents and rescues the impairment of the short-term memory in either 6- and 12-month-old 3×Tg-AD mice, respectively, with no significant effects on long-term memory. Moreover, insulin apparently exerts no significant effects on learning or memory in both adult and aged WT mice.

Intranasal Insulin Administration Ameliorates the Depressive-Like Behavior in 3×Tg-AD Mice

Depressive-like behaviors were measured by the tail suspension test (TST) and forced swim test (FST). Statistical details are reported in Supplementary Table 1. At 6 and 12 months of age, significant main effects of treatment, genotype, and genotype-by-treatment interactions were observed, except for the interaction in the older group of animals. As previously demonstrated [30, 31], post hoc comparisons revealed that the immobility time in both tests was

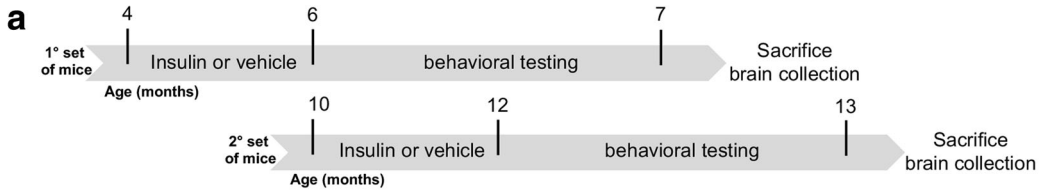
a
4
6
7
1° set of mice
Insulin or vehicle
behavioral testing
Sacrifice brain collection
Age (months)
10
12
13
2° set of mice
Insulin or vehicle
behavioral testing
Sacrifice brain collection
Age (months)

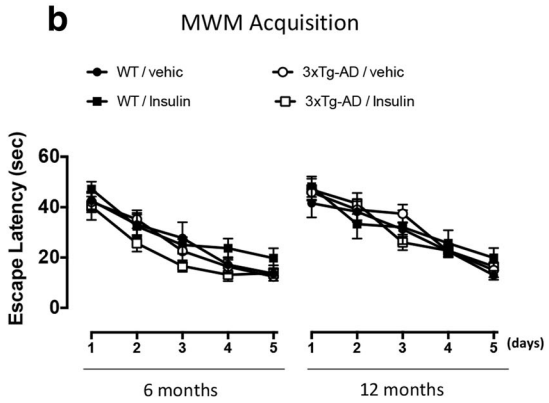
b
MWM Acquisition
WT / vehic
3xTg-AD / vehic
WT / Insulin
3xTg-AD / Insulin
Escape Latency (sec)
(days)
6 months
12 months

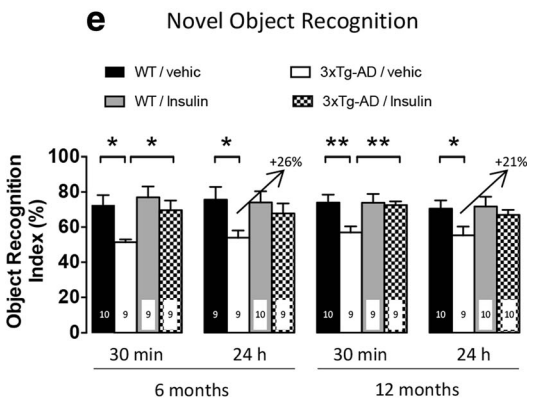
e
Novel Object Recognition
WT / vehic
3xTg-AD / vehic
WT / Insulin
3xTg-AD / Insulin
Object Recognition Index (%)
+26%
+21%
30 min
24 h
6 months
12 months

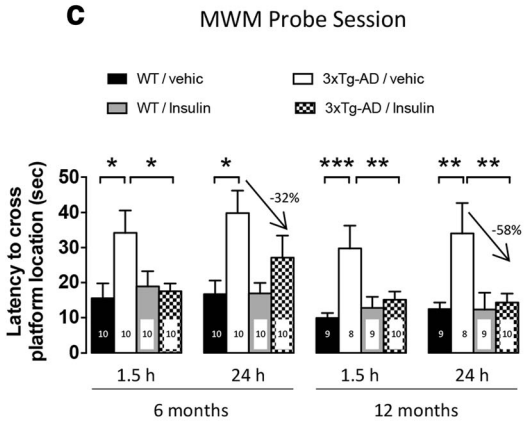
c
MWM Probe Session
WT / vehic
3xTg-AD / vehic
WT / Insulin
3xTg-AD / Insulin
Latency to cross platform location (sec)
-32%
-58%
1.5 h
24 h
6 months
12 months

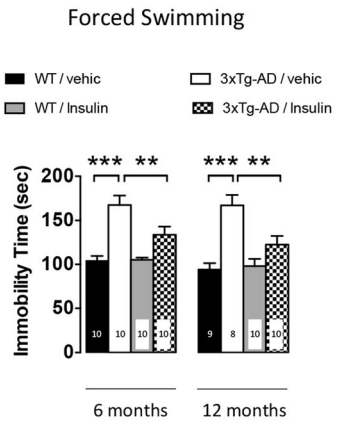
f
Forced Swimming
WT / vehic
3xTg-AD / vehic
WT / Insulin
3xTg-AD / Insulin
Immobility Time (sec)
6 months
12 months

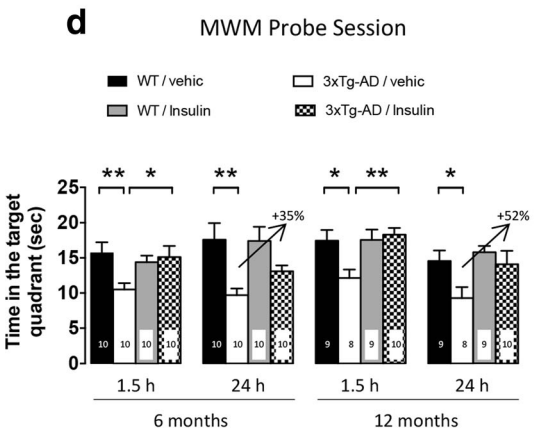
d
MWM Probe Session
WT / vehic
3xTg-AD / vehic
WT / Insulin
3xTg-AD / Insulin
Time in the target quadrant (sec)
+35%
+52%
1.5 h
24 h
6 months
12 months

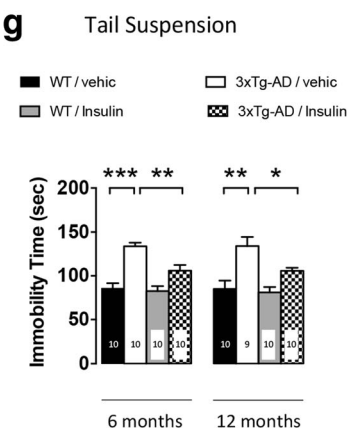
g
Tail Suspension
WT / vehic
3xTg-AD / vehic
WT / Insulin
3xTg-AD / Insulin
Immobility Time (sec)
6 months
12 months

◀ **Fig. 1** Insulin rescues short-term memory deficits and ameliorates the depressive-like phenotype in the 3×Tg-AD mice. **a** Schematic representation of the experimental design. Evaluation of the cognitive (**b**–**e**) and emotional phenotype (**f** and **g**) of 6- and 12-month-old 3×Tg-AD and age-matched non-Tg mice chronically treated with vehicle or insulin. Short- and long-term memory of mice was evaluated by **b**–**d** Morris water maze (MWM) and **e** novel object recognition (NOR) test (NORT). Moreover, the emotional phenotype of mice was evaluated by **f** forced swimming test (FST) and **g** tail suspension test (TST). Sample size is indicated in the bars. Data are presented as means ± SEM. Statistical analysis was performed by two-way ANOVA followed by Tukey's multiple comparison test (*$p < 0.05$; **$p < 0.01$; ***$p < 0.001$)

higher in vehicle-treated 3×Tg-AD than in vehicle-treated WT mice (Fig. 1f, g). Moreover, insulin significantly decreased the immobility time in the 3×Tg-AD mice for both tests, either at 6 and 12 months of age (Fig. 1f, g).

Taken together, these results confirm that 3×Tg-AD mice show a depressive-like phenotype, which is reversed by insulin treatment at 6 and 12 months of age. Moreover, insulin has no significant effect on WT mice.

Intranasal Insulin Administration Prevents the Impairment of BVR-A and the Early Dysfunction of the Insulin Signaling Cascade in Adult 3×Tg-AD Mice at 6 Months of Age

According to our hypothesis, the impairment of BVR-A is associated with the dysfunction of the insulin signaling cascade, which contributes to the cognitive impairment observed in AD [2, 39]. However, no data exist about the role of BVR-A in the hippocampal synaptic plasticity. To investigate this aspect, we studied long-term potentiation (LTP) at CA3–CA1 synapses in hippocampal organotypic slices biolistically transfected with shRNA for BVR-A together with a plasmid enconding enhanced green fluorescent protein (EGFP) to identify the transfected neurons (Fig. 2a). Silencing of BVR-A significantly reduced the LTP magnitude at CA3–CA1 synapses compared with LTP observed in neurons transfected with a scrambled shRNA (shLuc = 261 ± 92.4% vs shBVR-A = 176.9 ± 66.8%, $p = 0.049$; Fig. 2b).

These data demonstrate for the first time that BVR-A has a role in the hippocampal synaptic plasticity and therefore, its impairment in AD could be crucial to mediate cognitive and learning dysfunctions.

To determine whether INI administration was effective in preventing the impairment of BVR-A and the early alterations of the insulin signaling cascade observed in 3×Tg-AD mice at 6 months of age [12], here we evaluated changes of (i) BVR-A protein levels and Tyr phosphorylation together with (ii) the levels and activation of some main components of the insulin signaling cascade in the hippocampus and cortex of 3×Tg-AD mice and their littermate WT controls, treated with vehicle or insulin for 2 months (from 4 to 6 months of age). First, we confirmed our previous results showing reduced BVR-A

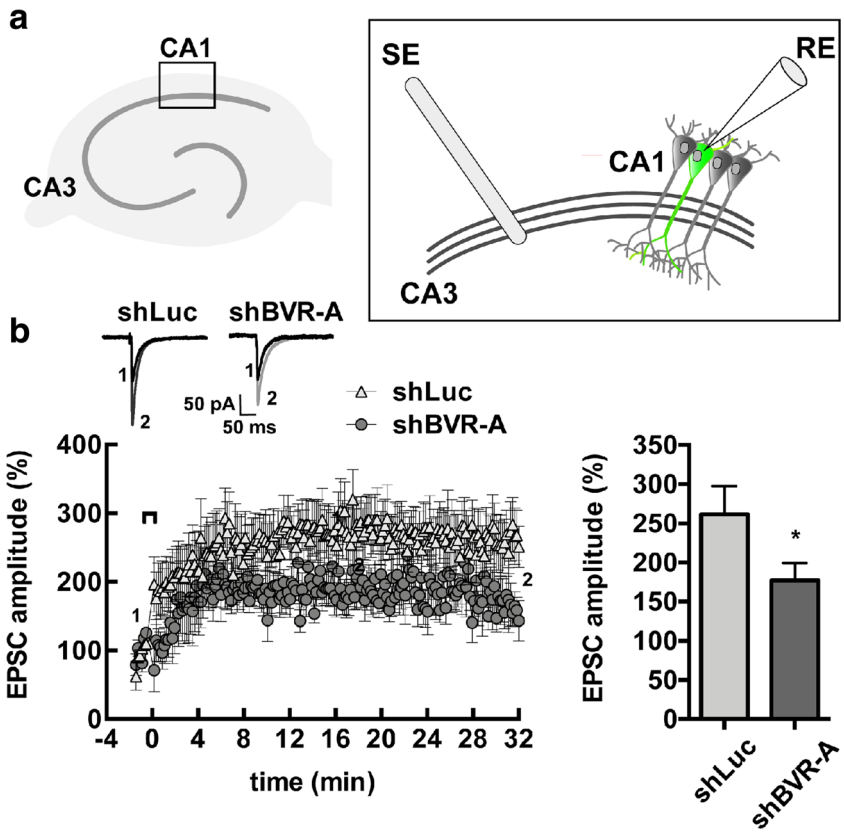

Fig. 2 Hippocampal LTP was inhibited in organotypic brain slices in which BVR-A was silenced. **a** Schematic representation of whole-cell recording from CA1 hippocampal pyramidal neuron in organotypic hippocampal slice (see methods for details). **b** Time course of LTP at CA3–CA1 synapses in hippocampal organotypic slices transfected with BVR-A shRNA or scrambled shRNA. Results are expressed as percentages of baseline EPSC amplitude (=100%). Insets (top) show representative EPSC at baseline (1) and during the last 5 min of LTP recording (2). **c** Mean LTP values during the last 5 min (n = 7–8/group). Data are expressed as mean ± SEM. *$p < 0.05$

levels and activation in the hippocampus of 6-month-old vehicle-treated 3×Tg-AD mice compared to vehicle-treated WT mice (Fig. 3a, c). INI treatment did not affect BVR-A protein levels (Fig. 3a, c), while INI was effective in preventing the observed impairment of BVR-A activation in 3×Tg-AD mice (Fig. 3b, c). No significant changes were observed between INI-treated and vehicle-treated WT mice (Fig. 3a–c).

Consistent with our hypothesis, the activation of BVR-A, induced by INI treatment, resulted in a significant

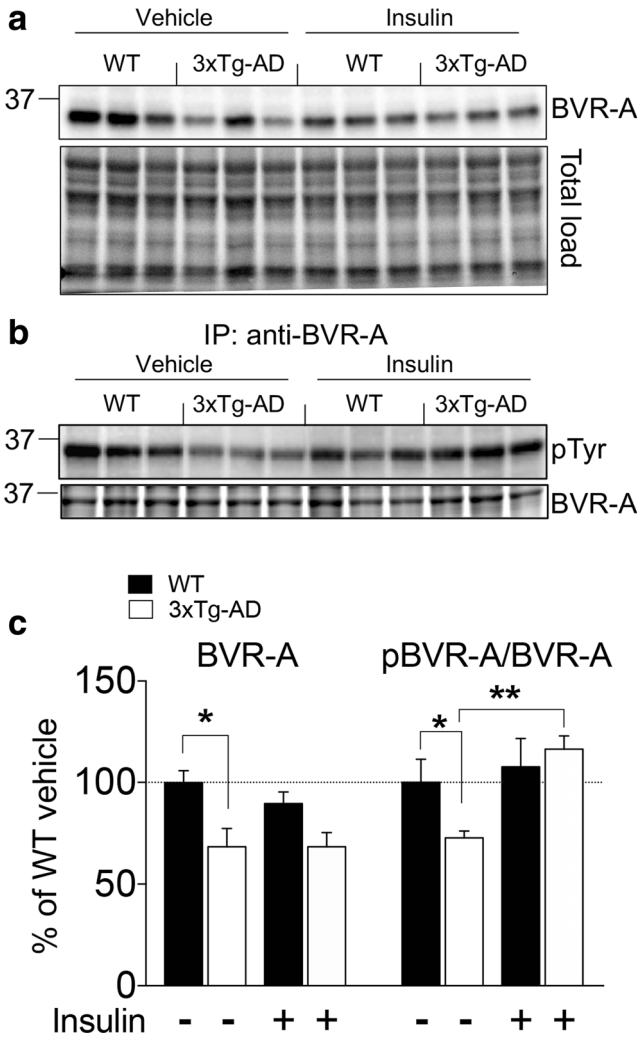

Fig. 3 Intranasal insulin prevents the early impairment of BVR-A in the hippocampus of 3×Tg-AD mice at 6 months of age. **a**, **b** Immunoblot analysis and **c** densitometric evaluation of changes of BVR-A protein levels and Tyr phosphorylation (pTyr) observed in the hippocampus of 3×Tg-AD mice and WT littermate controls treated with vehicle or insulin from 4 to 6 months of age. Densitometric values shown are given as percentage of WT mice vehicle set as 100%. BVR-A protein levels were normalized per total protein load. pTyr levels on BVR-A were normalized by using total BVR-A as loading control following immunoprecipitation [7, 38]. Data are presented as means ± SEM ($n = 6$ mice/group). Statistical analysis was performed by two-way ANOVA followed by Bonferroni's multiple comparison test (*$p < 0.05$). Pairwise comparisons available in Supplementary Table 2

improvement of the insulin signaling cascade in the hippocampus of 3×Tg-AD mice (Fig. 4). In particular, we found that INI further stimulated IR activation ($pIR^{Tyr1158/1161/1162}$/IR) in adult 3×Tg-AD mice compared to age-matched vehicle-treated 3×Tg-AD mice, leaving unchanged the IR protein levels (Fig. 4b, c). Moreover, we evaluated the activation of IRS1 by analyzing the levels of two of the best characterized sites known to promote IRS1 inhibition and thus insulin resistance even in AD brain: Ser307 and Ser636 [39, 40]. INI did not induce changes of IRS1 levels, while INI prevented the pathological hyper-activation of IRS1 in 3×Tg-AD mice, as demonstrated by the extent of IRS1 inhibition (mostly $pIRS1^{Ser636}$/IRS1), which returns close to those observed for WT mice (Fig. 4b, d). Rescue of the BVR-A/IRS1 axis activation was reflected by the activation of the downstream targets. Here, we extended our previous findings [12] by showing that ERK1/2 levels did not change across all the experimental groups, while their activation was significantly increased in the hippocampus of vehicle-treated 3×Tg-AD mice and it was partially reduced (~ 70%, $p = 0.07$) following INI administration (Fig. 5a, b). Further, we found that Akt protein levels in the hippocampus of 3×Tg-AD mice were significantly increased compared to vehicle-treated WT mice, and were not affected by INI treatment (Fig. 5a, c); conversely, Akt activation was strongly stimulated following insulin administration in 3×Tg-AD mice compared to vehicle-treated group ($pAkt^{Ser473}$/Akt, Fig. 5a, c). The improvement of Akt activation was associated with the amelioration of mTOR activation, whose reduction was prevented in INI-treated 3×Tg-AD mice ($p\text{-mTOR}^{Ser2448}$/mTOR, Fig. 5a, d). Keeping in mind the role of BVR-A in regulating insulin signaling at different levels [5, 8, 41], these observations further support our hypothesis that the impairment of BVR-A is associated upstream with the hyper-activation of the IR/IRS1 axis, while downstream with an aberrant activation of MAPK and Akt/mTOR axes. Instead, INI treatment prevents the alterations of BVR-A and ameliorates the entire activation of the insulin signaling in the hippocampus of adult 3×Tg-AD mice.

In WT mice, INI treatment led to a significant increase of the IR activation (Fig. 4c)—indicating the stimulatory effect of administered insulin—which was associated with a reduction of IRS1 Ser636 phosphorylation (~ 40%, $p = 0.06$, Fig. 4d), along with a significant increase of ERK1/2 activation (Fig. 5b). No changes of the Akt/mTOR pathway were observed in the hippocampus of INI-treated WT mice with respect to vehicle-treated WT mice (Fig. 5c, d). This is in agreement with the well-known possibility that the two main harms of the insulin signaling cascade, i.e., the MAPK and the Akt pathways, are not stimulated simultaneously [42, 43].

When we looked at the frontal cortex, we found that BVR-A protein levels were significantly reduced and were not associated with an impairment of BVR-A activation in adult vehicle-treated 3×Tg-AD mice with respect to WT mice

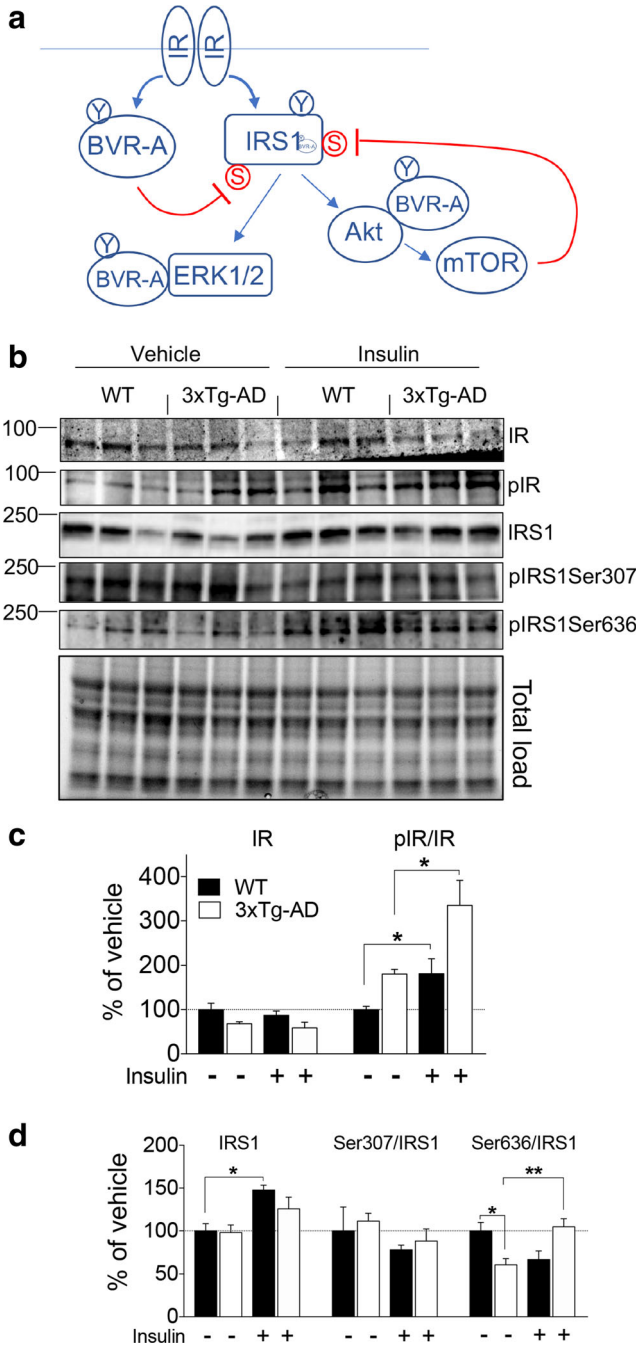

◀ **Fig. 4** Intranasal insulin prevents the hyper-activation of IRS1 in the hippocampus of 3 × Tg-AD at 6 months of age. **a** Schematic representation of the insulin signaling cascade. Blue arrows: activation; red line: inhibition; Y: tyrosine residues; S: serine residues. **b** Immunoblot analysis and **c**, **d** densitometric evaluation of IR and IRS1 protein levels and phosphorylation measured in the hippocampus of 3×Tg-AD mice and in WT littermate controls treated with vehicle or insulin from 4 to 6 months of age. Densitometric values shown are given as percentage of WT mice vehicle set as 100%. Protein levels were normalized per total protein load. Proteins' phosphorylation was normalized by taking into account the respective protein levels and are expressed as the ratio between the phosphorylated form and the total protein levels: $pIR^{(Tyr1158/1162/1163)}$/IR, $pIRS1^{(Ser307\ or\ Ser636)}$/IRS1. Data are presented as means ± SEM ($n = 6$ mice/group). Statistical analysis was performed by two-way ANOVA followed by Bonferroni's multiple comparison test ($*p < 0.05$, $**p < 0.01$). Pairwise comparisons available in Supplementary Table 2

(Supplementary Fig. 1C). Furthermore, no changes were observed following INI administration. Regarding the insulin signaling cascade, we observed an increased phosphorylation of the IR (Supplementary Fig. 2B) along with a significant increase of ERK1/2 activation (Supplementary Fig. 2D), possibly indicating an augmented basal activation of the MAPK pathway. However, no significant changes were observed for the other targets (e.g., Akt and mTOR). The observations about reduced BVR-A levels and increased IR activation in the frontal cortex of adult 3×Tg-AD mice recall the very early changes we found in the hippocampus of 3×Tg-AD mice at 3 months of age [12], thus suggesting that the alterations of the insulin signaling cascade do not progress at the same time and in the same way in different brain areas. INI administration did not promote significant changes for BVR-A or the activation of the insulin signaling in the frontal cortex of either adult 3×Tg-AD or WT mice (Supplementary Fig. 2).

Taken together, these lines of evidence suggest that the impairment of BVR-A occurs early along the progression of AD pathology in 3×Tg-AD mice and is associated with a dysfunction of the insulin signaling cascade mainly in the hippocampus, which can be significantly prevented by INI administration.

Intranasal Insulin Administration Recovers BVR-A Activation and Prevents the Onset of Brain Insulin Resistance in Aged 3×Tg-AD Mice at 12 Months of Age

To further characterize the molecular mechanisms underlying the beneficial effects of INI, we evaluated whether insulin treatment (from 10 to 12 months) was effective in recovering the activation of BVR-A and thus preventing the onset of brain insulin resistance in aged (12 months) 3×Tg-AD mice [12].

In agreement with what we observed with adult (6 months) 3×Tg-AD mice, INI administration to aged 3×Tg-AD mice did not promote changes of brain BVR-A protein levels, which remained reduced even after the treatment, whereas INI significantly recovered the activation of BVR-A in the hippocampus of aged 3×Tg-AD mice (Fig. 6a, c). Unexpectedly, INI treatment promoted a significant reduction of BVR-A activation in the hippocampus of WT mice compared to the vehicle-treated WT mice (Fig. 6a, c).

The evaluation of the insulin signaling cascade revealed that INI administration did not promote an increase of IR protein levels (Fig. 7a, b), while INI led to a consistent activation of the IR in the hippocampus of aged 3×Tg-AD mice compared to vehicle-treated 3×Tg-AD mice (Fig. 7a, b). With

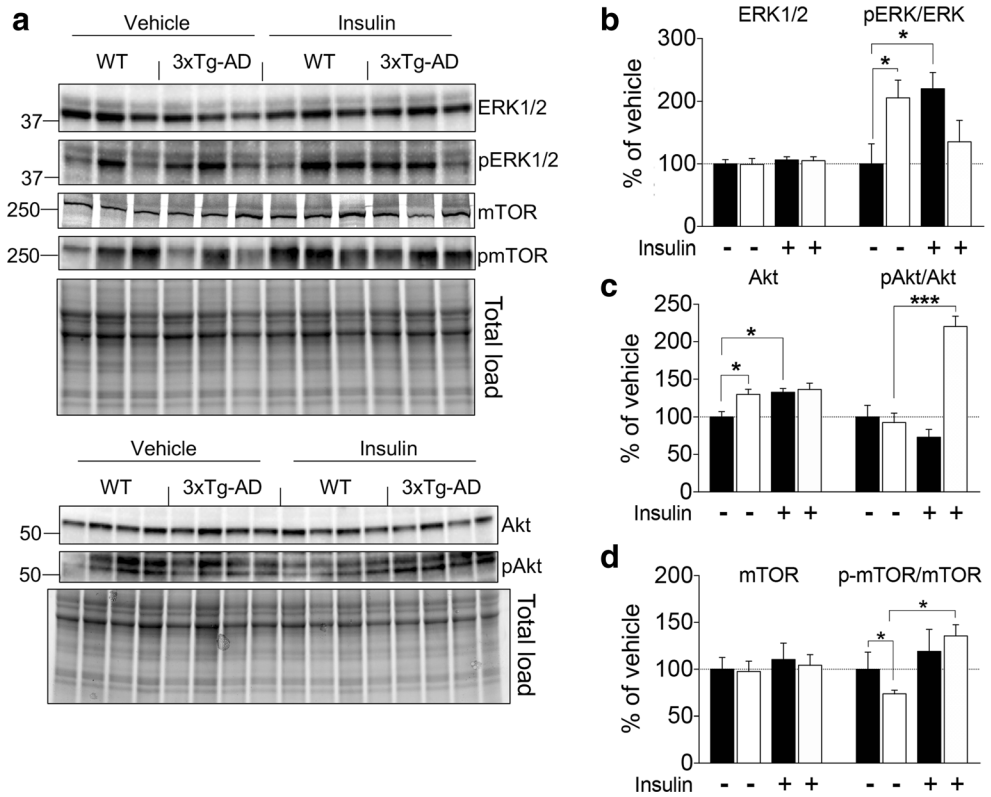

Fig. 5 Intranasal insulin prevents the early impairment of the insulin signaling cascade in the hippocampus of 3×Tg-AD at 6 months of age. (**a**) Immunoblot analysis and **b**–**d** densitometric evaluation of ERK1/2, Akt, and mTOR protein levels and phosphorylation measured in the hippocampus of 3×Tg-AD mice and in WT littermate controls treated with vehicle or insulin from 4 to 6 months of age. Densitometric values shown are given as percentage of WT mice vehicle set as 100%. Protein levels were normalized per total protein load. Proteins' phosphorylation was normalized by taking into account the respective protein levels and are expressed as the ratio between the phosphorylated form and the total protein levels: pERK1/2$^{(Thr202/Tyr204)}$/ERK1/2, pAkt$^{(Ser243)}$/Akt, pmTOR$^{(Ser2448)}$/mTOR. Data are presented as means ± SEM ($n = 6$ mice/group). Statistical analysis was performed by Two-way ANOVA followed by Bonferroni's multiple comparison test (*$p < 0.05$, **$p < 0.01$). Pairwise comparisons available in Supplementary Table 2

regard to IRS1 activation, here we strengthened our previous findings [12] by also showing a significant elevation of IRS1 Ser636 phosphorylation (Fig. 7a, c), which, together the observed impairment of the IR, are indicative of a condition of brain insulin resistance. INI significantly reduced the levels of IRS1 Ser636 phosphorylation in 3×Tg-AD mice, which were reported close to those of vehicle-treated WT mice (Fig. 7a, c). Downstream from IR, the amelioration of the BVR-A/IRS1 axis positively did impact on both ERK1/2 and Akt pathways in the hippocampus of aged 3×Tg-AD mice. Although we did not find changes for ERK1/2 or Akt protein levels (Fig. 8a–c), we found significant differences in terms of their activation. Indeed, the insulin resistance phenomenon was associated with no changes of ERK1/2 activation (Fig. 8a, b), but a consistent impairment of Akt activation in the hippocampus of vehicle-treated 3×Tg-AD mice was found (Fig. 8a, c). Strikingly, INI was effective in promoting the activation of both ERK1/2 (Fig. 8a, b) and Akt (Fig. 8a, c) proteins, thus indicating an improved insulin signaling activation. Downstream from Akt, we did not observe changes for mTOR protein levels and activation in aged 3×Tg-AD mice following INI treatment (Fig. 8a, d). However, by considering that IRS1 Ser636 is a direct target of mTOR when aberrantly activated [40], it seems that INI administration ameliorates the regulation of the Akt/mTOR axis finally resulting in a reduction of IRS1 Ser636 phosphorylation.

In WT mice, insulin administration promoted the activation of the IR without significant changes of the downstream targets, except for Akt whose activation was significantly reduced (Fig. 8a, c). Other than Akt, we also noticed an augmentation mTOR activation (~ 78%, $p = 0.08$, Fig. 8a, d), which, together with reduced BVR-A activation, could be representative of an impairment of the insulin signaling cascade. These results, therefore, possibly suggest that insulin, if administered for long time to an adult brain that is not compromised, could favor/accelerate the impairment of insulin signaling [as shown by [44–46]].

In the frontal cortex of aged 3×Tg-AD mice we observed changes that are in between those observed in the hippocampus of adult and aged 3×Tg-AD mice, further supporting a different temporal progression of the alterations of the insulin signaling between hippocampus and

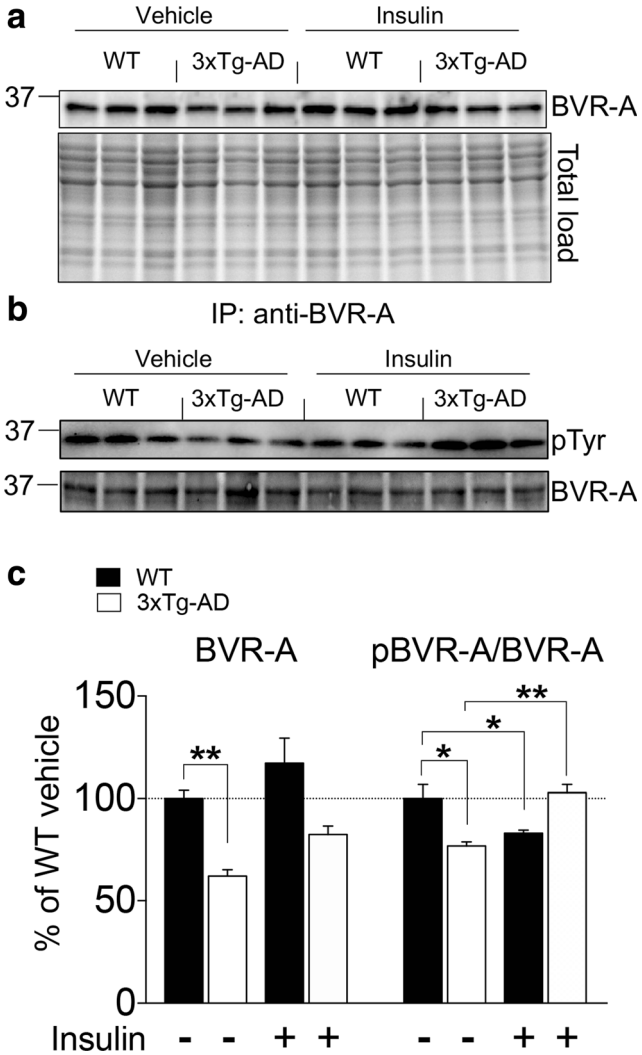

Fig. 6 Intranasal insulin recovers BVR-A activation in the hippocampus of 3×Tg-AD mice at 12 months of age. (**a**, **b**) Immunoblot analysis and **c** densitometric evaluation of changes of BVR-A protein levels and Tyr phosphorylation (pTyr) observed in the hippocampus of 3×Tg-AD mice and WT littermate controls treated with vehicle or insulin from 10 to 12 months of age. Densitometric values shown are given as percentage of WT mice vehicle set as 100%. BVR-A protein levels were normalized per total protein load. pTyr levels on BVR-A were normalized by using total BVR-A as loading control following immunoprecipitation [7, 38]. Data are presented as means ± SEM ($n = 6$ mice/group). Statistical analysis was performed by one-way ANOVA followed by Bonferroni's multiple comparison test (*$p < 0.05$; **$p < 0.01$). Pairwise comparisons available in Supplementary Table 2

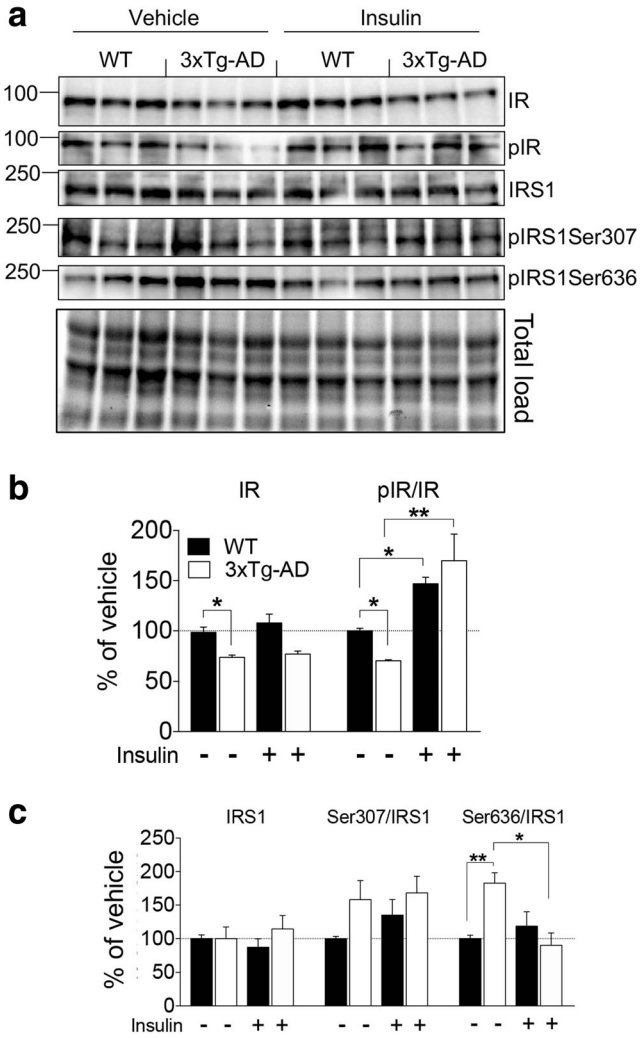

Fig. 7 Intranasal insulin promotes IR activation and prevents the inhibition of IRS1 in the hippocampus of 3×Tg-AD at 12 months of age. **a** Immunoblot analysis and **b**, **c** densitometric evaluation of IR and IRS1 protein levels and phosphorylation measured in the hippocampus of 3×Tg-AD mice and in WT littermate controls treated with vehicle or insulin from 10 to 12 months of age. Densitometric values shown are given as percentage of WT mice vehicle set as 100%. Protein levels were normalized per total protein load. Proteins' phosphorylation were normalized by taking into account the respective protein levels and are expressed as the ratio between the phosphorylated form and the total protein levels: $pIR^{(Tyr1158/1162/1163)}$/IR, $pIRS1^{(Ser307\ or\ Ser636)}$/IRS1. Data are presented as means ± SEM ($n = 6$ mice/group). Statistical analysis was performed by two-way ANOVA followed by Bonferroni's multiple comparison test (*$p < 0.05$; **$p < 0.01$). Pairwise comparisons available in Supplementary Table 2

cortex even in aged mice. We found a significant reduction of BVR-A levels and activation (Supplementary Fig. 3A,C) in the frontal cortex of vehicle-treated 3×Tg-AD mice with respect to vehicle-treated WT mice. INI treatment significantly improved only BVR-A activation (Supplementary Fig. 3A,C). With regard to the insulin signaling cascade, we observed a significant increase of IRS1 inhibition in vehicle-treated 3×Tg-AD mice with respect to WT mice (Supplementary Fig. 4A,C), without changes of the other components. Interestingly, INI led to a significant increase of IR activation (Supplementary Fig. 4A,B), and Akt activation (Supplementary Fig. 4A,E) in the 3×Tg-AD mice along with a decreasing trend of IRS1 inhibition (reduced Ser307 phosphorylation, ~ 80%, $p = 0.1$), which are all suggestive of an amelioration of the insulin signaling activation. No significant changes were observed for WT mice, regardless the treatment.

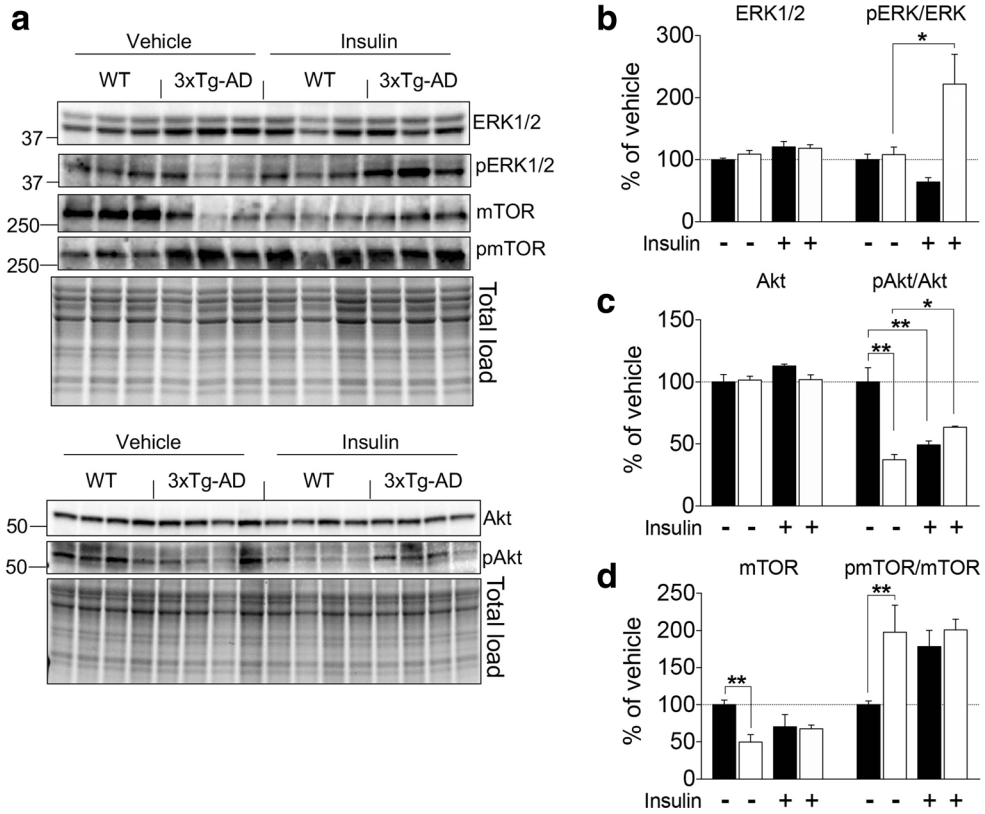

Fig. 8 Intranasal insulin promotes the activation of insulin cascade in the hippocampus of 3×Tg-AD at 12 months of age. **a** Immunoblot analysis and **b**–**d** densitometric evaluation of ERK1/2, Akt, and mTOR protein levels and phosphorylation measured in the hippocampus of 3×Tg-AD mice and in WT littermate controls treated with vehicle or insulin from 10 to 12 months of age. Densitometric values shown are given as percentage of WT mice vehicle set as 100%. Protein levels were normalized per total protein load. Proteins' phosphorylation were normalized by taking into account the respective protein levels and are expressed as the ratio between the phosphorylated form and the total protein levels: pERK1/2$^{(Thr202/Tyr204)}$/ERK1/2, pAkt$^{(Ser243)}$/Akt, pmTOR$^{(Ser2448)}$/mTOR. Data are presented as means ± SEM ($n = 6$ mice/group). Statistical analysis was performed by two-way ANOVA followed by Bonferroni's multiple comparison test (*$p < 0.05$; **$p < 0.01$). Pairwise comparisons available in Supplementary Table 2

Overall, these results suggest that INI administration improves the activation of BVR-A and prevents the onset of brain insulin resistance in the brain of aged 3×Tg-AD mice.

BVR-A Is Required for the Correct Transduction of the Insulin Signaling Cascade In vitro

To investigate whether BVR-A activation is essential to mediate the beneficial effects of the INI administration in 3×Tg-AD mice, we performed several in vitro experiments aimed to demonstrate that insulin's ability to recover cells from insulin resistance requires BVR-A. First, we tested whether insulin (100 nM) at different times (2–6–12–24 h) promotes the activation of its downstream targets in controls cells and in cells in which BVR-A had been silenced (to mimic a condition in which BVR-A does not work). We found that insulin leads to the activation of ERK1/2 and Akt only in control cells (Supplementary Fig. 5F and H, respectively). In siRNA-treated cells, insulin failed to promote its downstream effects. Rather, insulin treatment favors the inhibitory phosphorylation of IRS1 along with suppression of ERK1/2 and Akt activation (Supplementary Fig. 5F and H, respectively). These results, therefore, indicate that BVR-A is required to mediate the correct transduction of the insulin signaling cascade, which otherwise would be shifted toward a condition of insulin resistance. Based on these data and due to the fact that Akt was the main target modulated by the INI administration in 3×Tg-AD mice, we selected 2 h as time for treatment to use in the subsequent experiments. As shown in Fig. 9a, we set up a protocol in which, first, we induced insulin resistance and then we tried to recover insulin signaling activation both in control and siRNA-treated cells, by re-challenging these cells with increasing doses of insulin (to mimic the effect of the INI administration). Our data show that insulin mainly affects the activation of the selected targets since we did not observe significant changes of protein levels (Supplementary Fig. 6). Indeed, we found that insulin (100 nM, for 2 h) promoted the activation of IR, Akt, and mTOR in control cells (Fig. 9c–g, column 4), whereas a significant increase of IRS1 inhibition (Fig. 9d, column 5), a reduction of Akt activation

(Fig. 9f, column 5), and a sustained activation of mTOR (Fig. 9g, column 5) were observed when we induced insulin resistance by overexposing these cells to additional insulin (100 nM, for additional 2 h). Similar changes were found in siRNA-treated cells where insulin treatment (100 nM, 2 h) directly promoted insulin resistance (Fig. 9c–g, column 9). At this point, both control and siRNA-treated cells were rechallenged with fresh medium containing increasing doses of insulin (100 nM–500 nM–1 μM, for 2 h) to test whether insulin was able to recover the activation of the insulin signaling cascade. We found that insulin, at all the concentrations tested, further

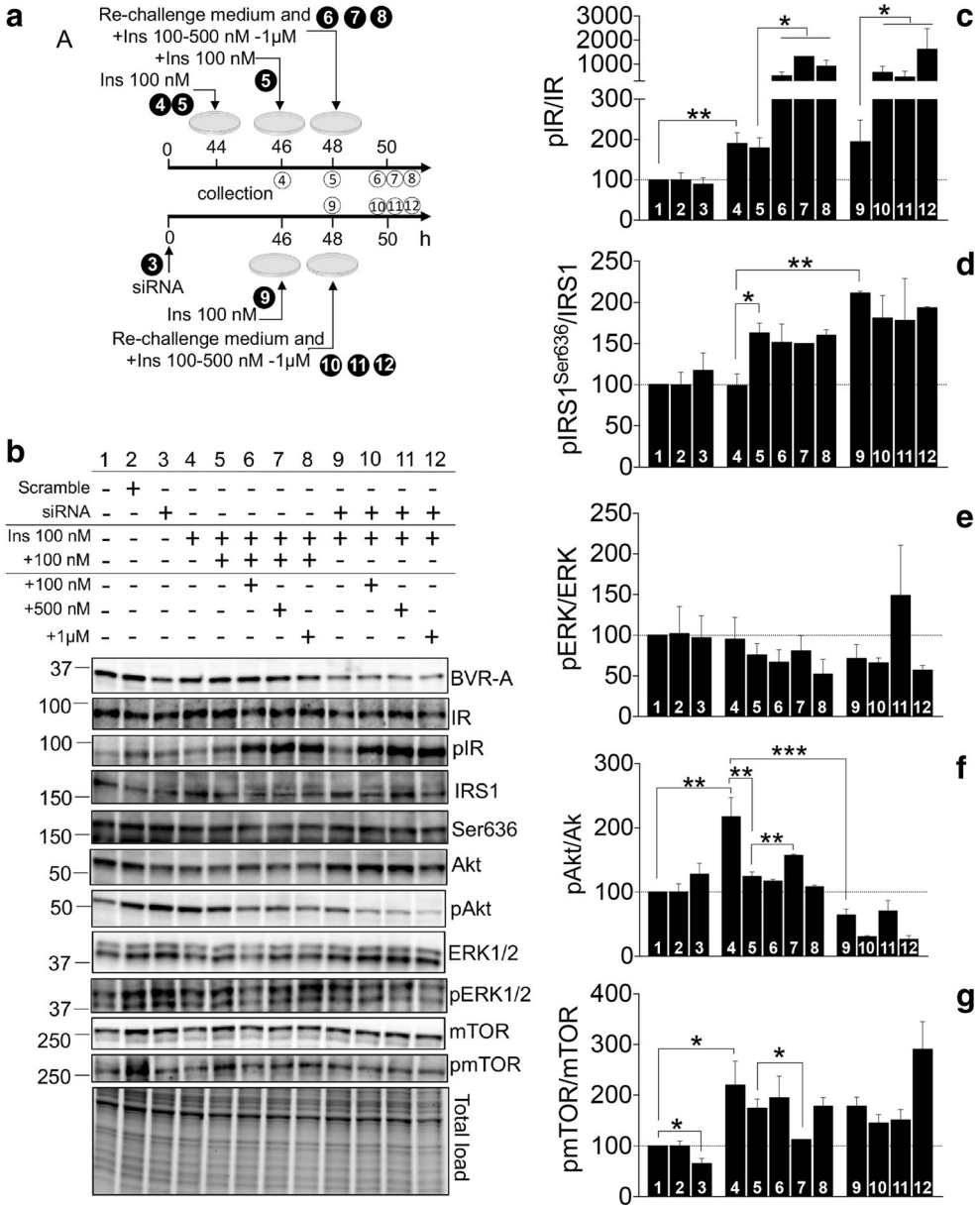

Fig. 9 BVR-A is required recovery insulin signaling activation in vitro. (**a**) Scheme of the protocol used to induce the activation of the insulin signaling as well as insulin resistance in HEK cells (for details see "Methods" section). For each condition, numbers in plain circle indicate the treatment while those in empty circle are relative the collection time. **b** Immunoblot analysis and **c**–**g** densitometric evaluation of BVR-A, IR, IRS1, ERK1/2, Akt, and mTOR activation evaluated following different insulin treatments in control HEK cells or in cells in which BVR-A was silenced through a specific siRNA. Numbers in panel (**b**) and those indicated in each column of the densitometric analysis are matched and are indicative of the treatment performed as also indicated in (**a**). Densitometric values shown are given as percentage of control cells (column 1) set as 100%. Protein levels were normalized per total protein load. Proteins' phosphorylation were normalized by taking into account the respective protein levels and are expressed as the ratio between the phosphorylated form and the total protein levels: $pIR^{(Tyr1158/1162/1163)}$/IR, $pIRS1^{(Ser636)}$/IRS1, $pERK1/2^{(Thr202/Tyr204)}$/ERK1/2, $pAkt^{(Ser243)}$/Akt, $pmTOR^{(Ser2448)}$/mTOR. Data are presented as means ± SEM ($n = 3$ independent cultures/group). *$p < 0.05$ (Student t test)

increased the activation of IR both in control (Fig. 9c, columns 6–8) and siRNA-treated cells (Fig. 9c, columns 10–12). Notwithstanding this result, we observed a difference in terms of activation of the downstream targets. In control cells, among the tested doses, insulin at 500 nM was able to partially recover the activation of Akt (Fig. 9f, column 7), thus possibly indicating an amelioration of the insulin signaling cascade. Conversely, neither of the tested doses was effective in promoting Akt activation in siRNA-treated cells (Fig. 9f, columns 10–12). Increased Akt activation was also associated with a reduction of mTOR activation in control cells (Fig. 9g, column 7). Instead, a persistent mTOR activation even further elevated at the highest dose of insulin (1 μM) was observed in cells in which BVR-A was silenced (Fig. 9g, columns 10–12). Also in this case, we did not observe significant changes of protein levels (Supplementary Fig. 7).

To further confirm the pivotal role of BVR-A, we took advantage of the use of the BVR-A mimetic peptide ^{290}KYCCSRK, which has been previously demonstrated to mimic the kinase activity of BVR-A toward the IR/IRS1 axis, thus favoring the activation of the insulin signaling cascade [6, 47]. Strikingly, we found that insulin (100 nM, for 2 h) did not induce insulin resistance if administered together with the peptide (10 and 20 μM) in siRNA-treated cells (Fig. 10, columns 5–7). The treatment with the peptide at both the tested doses favors the activation of the insulin signaling cascade as demonstrated by the significant reduction of IRS1 inhibition (Fig. 10d, columns 6–7), the increase of both ERK1/2 (Fig. 10e, columns 6–7) and Akt activation (Fig. 10f, columns 6–7) and the reduction of mTOR activation (Fig. 10g, columns 6–7). Furthermore, the peptide allows recovery of siRNA-treated cells from insulin resistance (Fig. 10, columns 8–10). Indeed, while insulin alone is not able to recover insulin signaling activation, insulin does if administered together with the peptide, which leads to a significant reduction of IRS1 inhibition (Fig. 10d, columns 8–10) along with a significant activation of Akt (Fig. 10f, columns 8–10) and a reduction of mTOR activation (Fig. 10g, columns 8–10).

Overall, these findings demonstrate the central role that BVR-A plays in the regulation of the insulin signaling cascade and also strengthen the notion of the role played by BVR-A in the molecular mechanisms underlying the beneficial effects of the INI administration.

Amelioration of Insulin Signaling Activation Is Associated with Reduced Oxidative Stress Levels and AD Neuropathological Markers in the Hippocampus and Cortex of INI-Treated 3×Tg-AD Mice

We previously reported that the dysregulation of the insulin signaling cascade in the hippocampus of 3×Tg-AD mice was associated with increased oxidative/nitrosative stress levels as well as a worsening of AD-like neuropathology [12]. To further explore whether the improved functionality of the insulin signaling cascade following INI administration might affect the abovementioned pathological features of AD brain, we evaluated changes of oxidative/nitrosative stress markers, Aβ oligomers and Tau levels, and phosphorylation in the hippocampus and cortex of WT and 3×Tg-AD mice both at 6 and 12 months of age.

We found that INI treatment significantly reduced 3-NT levels in the hippocampus both in adult (Fig. 11a) and aged (Fig. 11b) 3×Tg-AD mice. In agreement with data about the activation of the insulin signaling cascade following INI administration, a reduction of 3-NT levels close to significance was found in the cortex of adult 3×Tg-AD mice (~ 75%, $p = 0.06$, Supplementary Fig. 8).

In parallel, western blot analysis revealed that INI treatment did not significantly modify the expression of full-length APP and Aβ dodecamer (Aβ*56) either in the hippocampus or in frontal cortex of 6-month-old insulin-treated 3×Tg-AD mice (Fig. 12a, b and Supplementary Fig. 8B-C, respectively). Rather, we observed a significant reduction of Aβ oligomers in hippocampus (Fig. 12c, d) but not in frontal cortex of 12-month-old 3×Tg-AD (Supplementary Fig. 8E-F). To better understand the mechanisms responsible for the observed reduction of Aβ in the hippocampus of 3×Tg-AD mice following INI administration, we analyzed the expression levels of the insulin-degrading enzyme (IDE), known to be involved in the degradation of Aβ [48]. Regardless of the age of the mice, we observed no significant changes in the expression levels of IDE either in the hippocampus or cortex of 3×Tg-AD mice after INI administration (Fig. 12a, b and Supplementary Fig. 8E-F), thus suggesting that probably other degradative or clearance mechanisms are responsible for the observed reduction of Aβ oligomers.

Finally, we found that INI administration was able to ameliorate Tau pathology both in hippocampus and frontal cortex of 3×Tg-AD mice. In particular, we observed reduced phosphorylation levels of tau protein on Ser202/Thr205 residues in the hippocampus of adult (Fig. 12a, b) and aged (Fig. 12c, d) 3×Tg-AD mice, as well as in the frontal cortex of aged 3×Tg-AD mice (Supplementary Fig. 8E-F).

Discussion

With a long prodromal period of 10 to 20 years, AD and related dementias are becoming a priority for many governments, considering that 1% of global gross domestic product is spent on dementia care [49]. Brain insulin resistance greatly contributes to this preclinical period during which only subtle behavioral symptoms are evident [25], and no reliable biomarkers indicative of any potential risks are available [50].

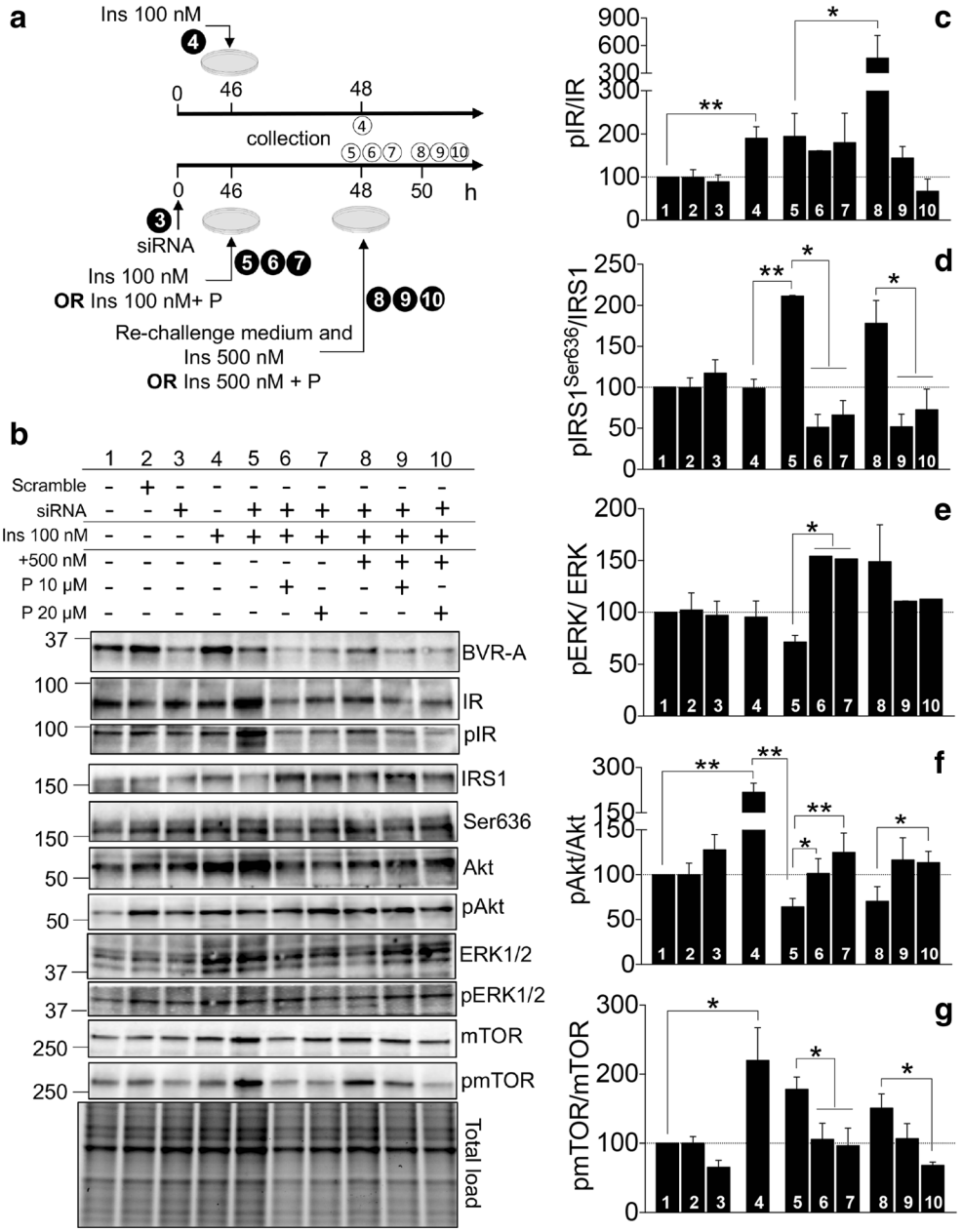

Fig. 10 The BVR-A mimetic peptide ^{290}KYCCSRK recovers the correct activation of the insulin signaling cascade in cells lacking BVR-A. **a** Scheme of the protocol used to treat cells (for details see "Methods" section). For each condition, numbers in plain circle indicate the treatment while those in empty circle are relative the collection time. **b** Immunoblot analysis and **c**–**g** densitometric evaluation of BVR-A, IR, IRS1, ERK1/2, Akt, and mTOR activation evaluated in control cells or in cells silenced for BVR-A and treated with insulin alone or in combination with the ^{290}KYCCSRK peptide (P). Numbers in panel (**b**) and those indicated in each column of the densitometric analysis are matched and are indicative of the treatment performed as also indicated in (**a**). Densitometric values shown are given as percentage of control cells (column 1) set as 100%. Protein levels were normalized per total protein load. Proteins' phosphorylation were normalized by taking into account the respective protein levels and are expressed as the ratio between the phosphorylated form and the total protein levels: pIR$^{(Tyr1158/1162/1163)}$/IR, pIRS1$^{(Ser636)}$/IRS1, pERK1/2$^{(Thr202/Tyr204)}$/ERK1/2, pAkt$^{(Ser243)}$/Akt, pmTOR$^{(Ser2448)}$/mTOR. Data are presented as means ± SEM ($n = 3$ independent cultures/group). *$p < 0.05$ and **$p < 0.01$ (Student t test)

Therefore, the comprehension of the initiating molecular events leading to brain insulin resistance is fundamental to strengthen the setup of new prevention strategies aimed to reduce both the risks and the dramatic outcomes of metabolic dysfunctions in the brain.

We show for the first time that alterations of the insulin signaling cascade do not occur simultaneously in different brain areas. Our data are supportive for a different progression between hippocampus and frontal cortex. Indeed, hippocampus shows a marked alteration of the insulin signaling before

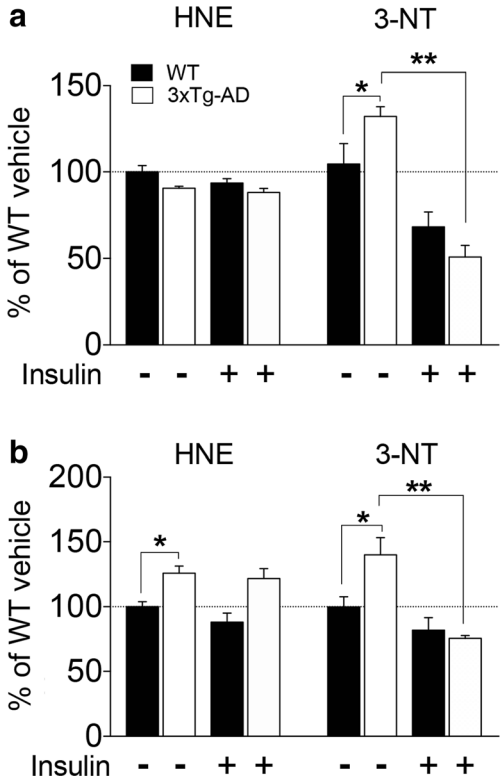

Fig. 11 Improvement of insulin signaling cascade activation following insulin administration is associated with reduced nitrosative stress levels in the hippocampus of 3×Tg-AD mice. Changes of oxidative (HNE) and nitrosative (3-NT) stress levels evaluated in the hippocampus of 3×Tg-AD mice and WT littermate controls treated with vehicle or insulin from (**a**) 4 to 6 months and (**b**) from 10 to 12 months of age. Data shown are given as percentage of WT mice vehicle set as 100%. Data are presented as means ± SEM ($n = 6$ mice/group). Statistical analysis was performed by two-way ANOVA followed by Bonferroni's multiple comparison test (*$p < 0.05$; **$p < 0.01$). Pairwise comparisons available in Supplementary Table 2

the frontal cortex both in adult and aged 3×Tg-AD mice. This is in line with the temporal development of AD neuropathology in the brain of 3×Tg-AD mice [26, 51–53].

Then, to better characterize the molecular mechanisms underlying the alterations of brain insulin signaling, we focused on the protein BVR-A [41], whose impairment was demonstrated to precede the canonical molecular alterations associated with the insulin resistance phenomenon, i.e., reduced IR or increased IRS1 inhibition [39, 42, 54, 55] in 3×Tg-AD mice [12]. Indeed, as previously reported by our and Butterfield's group, BVR-A is consistently impaired in human mild cognitive impairment (MCI) and AD hippocampus [10, 11, 56] known to be characterized by increased IRS1 inhibition and mTOR hyper-activation [57]. Similarly, reduced BVR-A activation was found in plasma samples collected from AD MCI and AD patients [58]. Furthermore, reduced BVR-A levels and activation have been found in the hippocampus of 3×Tg-AD mice before IRS1 inhibition and analogous changes have been observed in WT mice with age [12]. In addition, a dysfunction of BVR-A has been observed in the parietal cortex of beagles—who spontaneously deposit human-type amyloid β (Aβ) peptide [59, 60] and thus are a natural higher mammalian model of aging than rodents—quite early during the aging process along with a reduced activation of the insulin signaling cascade [61]. Based on these lines of evidence, we believe that the impairment of BVR-A is an event which precedes the development of brain insulin resistance.

Hence, we hypothesized that INI administration, by favoring the IR-mediated activation of BVR-A, would prevent the alterations of the insulin signaling in the brain. Indeed, despite the reported beneficial effects of INI administration in humans [14–16, 62, 63], the molecular mechanisms that underlie the effects of insulin are still poorly understood. In particular, it is not clear whether or not intranasal insulin overcomes insulin resistance by promoting the activation of the insulin signaling cascade [25, 64].

Here, we provided some answers to this point by demonstrating that INI treatment promoted the activation of the IR and its downstream targets in the brain of both adult and aged 3×Tg-AD mice. Remarkably, improvement of insulin signaling activation occurs along with an improvement of BVR-A activation both in the hippocampus and cortex.

In agreement with our hypothesis, INI administration prevented the early impairment of BVR-A activation in 3×Tg-AD mice (Fig. 3). Indeed, an improved BVR-A activation seems to be useful to dampen IRS-1 hyper-activation (as indexed by decreased Ser636 phosphorylation) (Fig. 4d), and it is also associated with an improvement of Akt phosphorylation (Fig. 5c) [8], which also prevents the failure of mTOR activation (Fig. 5d), in the hippocampus of 3×Tg-AD mice at 6 months of age.

As previously reported, other than the brain insulin resistance phenomenon, also this non-physiological hyper-activation phase could produce deleterious effects in terms of learning and memory functions [65–69]. Interestingly, by preventing the early alterations of the insulin signaling cascade in the 6-month-old 3×Tg-AD mice, INI also significantly ameliorated the short-term spatial learning in MWM, as well as the short-term working memory in the NOR task (Fig. 1). Differently, the long-term memory (spatial and working) was not significantly affected by INI treatment, although we observed a trend toward an improvement of cognitive dysfunctions compared to vehicle-treated 3×Tg-AD mice. Other authors found that INI treatment was able to positively affect the long-term memory in C57BL/6 mice [70]. The discrepancy may be attributed to the differences in the experimental contexts and animals (transgenic vs non-transgenic mice, adult/aged vs very young), and mostly due to the use of different dosage of insulin and scheme of treatment (80 μg/every other day for 2 months vs 900 μg/day for 7 days), which may have affected the assessment of the cognitive phenotype in our experiments versus those reported by other authors.

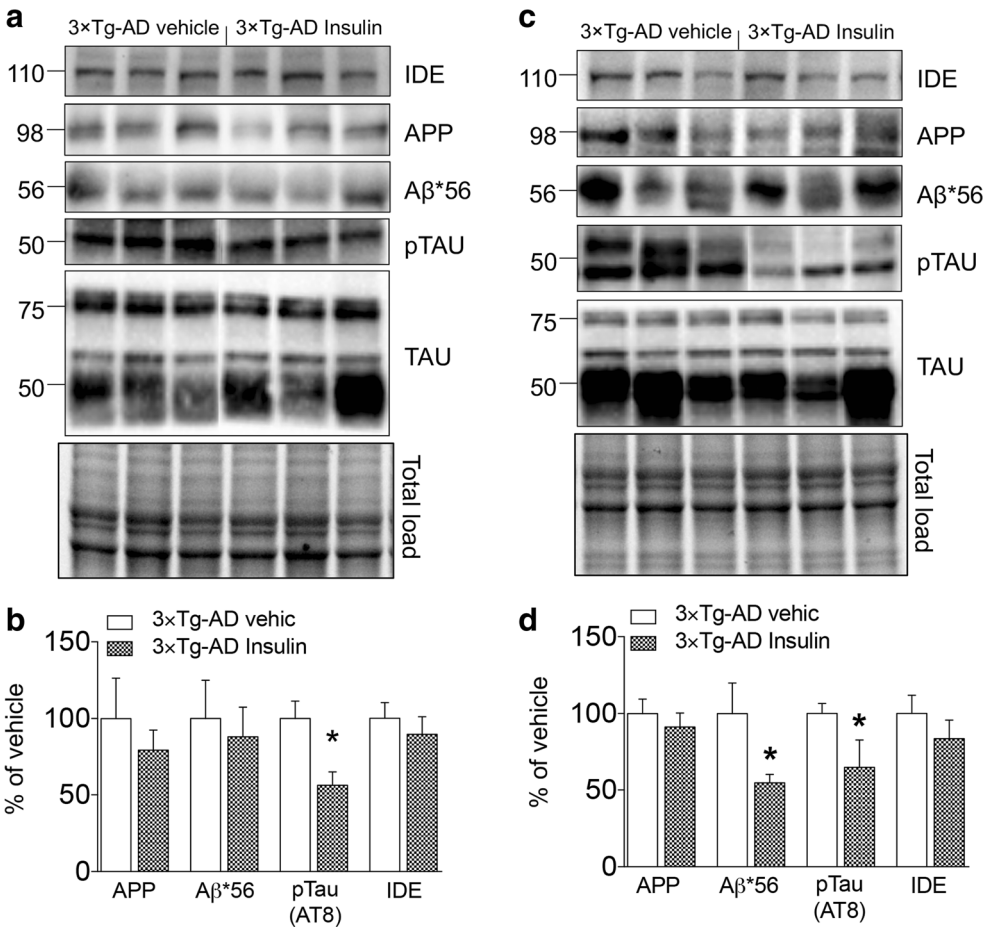

Fig. 12 Improvement of insulin signaling cascade activation following insulin administration is associated with an amelioration of AD neuropathology in the hippocampus of 3×Tg-AD mice. **a**, **c** Immunoblot analysis and **b**, **d** densitometric evaluation of changes of full-length APP, Aβ dodecamer (Aβ*56), Tau phosphorylation and IDE measured in the hippocampus of 3×Tg-AD treated with vehicle or insulin from 4 to 6 months (**a**, **b**) and from 10 to 12 months (**c**, **d**) of age. Densitometric values shown are given as percentage of 3×Tg-AD mice vehicle set as 100%. Protein levels were normalized per total protein load. Tau phosphorylation was normalized by taking into account the respective protein levels and are expressed as the ratio between the phosphorylated form and the total protein levels: $pTau^{(Ser202/Thr205)}$/Tau. Data are presented as means ± SEM ($n = 6$ mice/group). *$p < 0.05$ (Student t test)

Also of interest, to our knowledge, this is the first study showing that INI treatment ameliorates depressive-like behavior in the 6-month-old 3×Tg-AD mice performing two different tests (Fig. 1). It is prudent, in fact, to test parallel depressive paradigms to strongly confirm phenotype. We therefore decided to perform two subsequent tests that are indicators of depressive behavior: forced swimming and tail suspension. We previously demonstrated that 3×Tg-AD mice show a depressive-like phenotype [30, 31] that is completely reversed by INI treatment.

Collectively, these observations agree with the well-known role of insulin in modulating synaptic plasticity [that is, LTP and long-term depression (LTD)] via Akt [42, 71]. Furthermore, insulin has a crucial role in the development and maintenance of excitatory synapses [42, 72] and has been shown to promote dendritic spine formation and excitatory synapse development through activation of the Akt/mTOR axis [42, 73]. In this picture, our results showing that silencing of BVR-A is sufficient to promote a dysfunction of LTP in rat brain slices (Fig. 2) represent an intriguing novelty, that, together with the observed impairment of the insulin signaling, further supports a role for BVR-A in the molecular mechanisms regulating cognitive functions (Fig. 1).

The effectiveness of INI administration is evident also in aged (12 months of age) 3×Tg-AD mice used to test the hypothesis that INI, by rescuing BVR-A impairment, prevents the onset of brain insulin resistance. Indeed, at 12 months of age these mice show a reduction of BVR-A activation along with clearly signs of insulin resistance including (i) reduced IR levels and activation (Fig. 7b), (ii) increased IRS1 Ser636 phosphorylation (Fig. 7c), and (iii) uncoupling of Akt/mTOR signaling (Fig. 8c, d). Interestingly, we found that INI treatment was able to recover the activation of BVR-A (Fig. 6) and to prevent the increased IRS1 inhibition (Fig. 7c), which results in a downstream improvement of both Akt (Fig. 8c) and ERK1/2 activation (Fig. 8b), finally leading to a significant recovery in terms of cognitive functions (Fig. 1) [1, 2, 42, 74]. In fact, at the behavioral level, 12-month-old 3×Tg-AD mice confirm the phenotype of younger 3×Tg-AD mice. In particular, INI treatment significantly enhances short-term spatial and working memory, as well as evokes depressive-like behavior in 3×Tg-AD mice (Fig. 1). As far as the long-term memory, INI treatment significantly decreases (− 58%) the latency to cross platform location in the MWM and, although not significant, also ameliorates other behavioral endpoints of spatial and working memory in the

3×Tg-AD mice compared to age-matched, vehicle-treated 3×Tg-AD mice.

Surprisingly, we did not see a decrease of mTOR activation—which is among the kinases whose aberrant activity is known to mediate IRS1 inhibition [40, 75] also in AD [3, 76–80]—in aged 3×Tg-AD mice following insulin treatment. However, we believe that the improvement of Akt activation together with the observed decrease of IRS1 phosphorylation on a site known to be target of mTOR kinase activity [Ser636 [40]] are indicative of an improved regulation of the Akt/mTOR axis.

All these lines of evidence suggest that changes of BVR-A are strongly associated with alterations of the insulin signaling cascade in the brain. However, whether BVR-A is directly involved in the beneficial effects of INI both in adult and aged mice remained to be investigated. For that reason, we performed several in vitro experiments by using cells in which BVR-A was silenced to clarify the role of BVR-A in the mechanisms associated with insulin resistance (Figs. 9 and 10). First, our results demonstrated that cells lacking BVR-A and treated with insulin develop insulin resistance rather than a physiological activation of the insulin signaling (Supplementary Fig. 5 and Fig. 7). Indeed, an increase of IRS1 Ser636 phosphorylation (Fig. 9d, column 5), a decrease of Akt activation (Fig. 9f, column 5) along with a persistent activation of mTOR (Fig. 9g, column 5) was observed. Interestingly, these results agree with the molecular changes observed in 3×Tg-AD mice at 12 months of age (Figs. 7 and 8). At that age, we showed that BVR-A is required to recover cells from insulin resistance (Fig. 9), since the above-cited alterations were retrieved only in control cells but not in cells lacking BVR-A, following the exposure to high dose insulin (500 nM) (Fig. 9). These data, therefore, strongly support the mechanism hypothesized for INI-treated mice. The essential role for BVR-A is strengthened by the results collected in cells lacking BVR-A and treated with a BVR-A mimetic peptide (Fig. 10). Several sequence motifs within BVR-A structure were identified as possible protein–protein interaction sites: the cysteine-containing ^{275}KKRILHC and ^{290}KYCCSRK in the C-terminal α-helix, and the two SH2-binding motifs (^{198}YMKM and ^{228}YLSF) [36]. Among these peptides, ^{290}KYCCSRK was found to stimulate IR-mediated phosphorylation/activation of BVR-A finally leading to an increase glucose uptake in HEK cells [6, 47]. However, these observations were limited to the evaluation of basal glucose uptake. Thus, we tested whether the ^{290}KYCCSRK peptide could rescue cells from insulin resistance, and we demonstrated that in cells lacking BVR-A insulin promotes the activation of the insulin signaling cascade, and thus recoveries cells from insulin resistance, only if administered together with the peptide (Fig. 10). Indeed, decreased IRS1 inhibition, increased ERK1/2 and Akt activation, and decreased mTOR hyperactivity were observed (Fig. 10).

The recovery of insulin signaling physiological activation in 3×Tg-AD mice had beneficial effects also on Aβ and Tau pathology and is able to reduce the accumulation of oxidative damage both in adult and aged 3×Tg-AD mice (Fig. 11). Accordingly, previous data demonstrated that insulin deficiency leads to increased Tau phosphorylation, which was reversed by insulin administration directly in the brain [81–84], and that higher brain insulin concentrations may reduce amyloid oligomerization and toxicity [85], increase synaptogenesis [86], or modulate long-term potentiation and depression in the hippocampus, thus improving learning and memory [87].

Taken together, these findings propose that the dysfunction of BVR-A is an early event in the development of brain insulin resistance and that by recovering BVR-A activity, it is possible both to rescue early alterations of the insulin signaling cascade and to prevent the onset of brain insulin resistance. So far, most of the studies have been aimed to understand the factors that mediate IRS1 inhibition or determine means to recovery IRS1 activation. However, when IRS1 is significantly inhibited, it is already late. Strikingly, our results represent a step forward for the comprehension of the very early mechanisms responsible for the alteration of the insulin signaling cascade, finally resulting in brain insulin resistance. The comprehension of the initiating molecular events is fundamental to develop new prevention strategies and to improve therapeutic strategies for the treatment of AD. Among the latter, is the intranasal insulin administration, with the final goal to reduce the risks and impact of brain metabolic alterations in an aging population. Our work contributed to this goal.

Author Contribution EB, TC, and MP designed the study. EB, AT, FT, SC, and FDD performed the mouse experiments. TC and SG performed the behavioral tests. CR performed the electrophysiology experiments. EB, TC, MP, CG, and DAB analyzed and interpreted the data. EB and MP drafted the manuscript. All authors revised the manuscript critically for important intellectual content and approved the final version.

Compliance with Ethical Standards

Conflict of interest The authors declare that they have no conflict of interest.

Publisher's Note Springer Nature remains neutral with regard to jurisdictional claims in published maps and institutional affiliations.

References

1. De Felice FG (2013) Alzheimer's disease and insulin resistance: translating basic science into clinical applications. J Clin Invest 123(2):531–539. https://doi.org/10.1172/JCI64595
2. Biessels GJ, Reagan LP (2015) Hippocampal insulin resistance and cognitive dysfunction. Nat Rev Neurosci 16(11):660–671. https://doi.org/10.1038/nrn4019

3. Tramutola A, Triplett JC, Di Domenico F, Niedowicz DM, Murphy MP, Coccia R, Perluigi M, Butterfield DA (2015) Alteration of mTOR signaling occurs early in the progression of Alzheimer disease (AD): analysis of brain from subjects with pre-clinical AD, amnestic mild cognitive impairment and late-stage AD. J Neurochem 133(5):739–749. https://doi.org/10.1111/jnc.13037
4. Taniguchi CM, Emanuelli B, Kahn CR (2006) Critical nodes in signalling pathways: insights into insulin action. Nat Rev Mol Cell Biol 7(2):85–96. https://doi.org/10.1038/nrm1837
5. Lerner-Marmarosh N, Shen J, Torno MD, Kravets A, Hu Z, Maines MD (2005) Human biliverdin reductase: a member of the insulin receptor substrate family with serine/threonine/tyrosine kinase activity. Proc Natl Acad Sci U S A 102(20):7109–7114. https://doi.org/10.1073/pnas.0502173102
6. Gibbs PE, Lerner-Marmarosh N, Poulin A, Farah E, Maines MD (2014) Human biliverdin reductase-based peptides activate and inhibit glucose uptake through direct interaction with the kinase domain of insulin receptor. FASEB J 28(6):2478–2491. https://doi.org/10.1096/fj.13-247015
7. Lerner-Marmarosh N, Miralem T, Gibbs PE, Maines MD (2008) Human biliverdin reductase is an ERK activator; hBVR is an ERK nuclear transporter and is required for MAPK signaling. Proc Natl Acad Sci U S A 105(19):6870–6875. https://doi.org/10.1073/pnas.0800750105
8. Miralem T, Lerner-Marmarosh N, Gibbs PE, Jenkins JL, Heimiller C, Maines MD (2016) Interaction of human biliverdin reductase with Akt/protein kinase B and phosphatidylinositol-dependent kinase 1 regulates glycogen synthase kinase 3 activity: a novel mechanism of Akt activation. FASEB J 30(8):2926–2944. https://doi.org/10.1096/fj.201600330RR
9. Zhang Y, Zong W, Zhang L, Ma Y, Wang J (2016) Protein kinase M zeta and the maintenance of long-term memory. Neurochem Int 99:215–220. https://doi.org/10.1016/j.neuint.2016.07.007
10. Barone E, Di Domenico F, Cenini G, Sultana R, Coccia R, Preziosi P, Perluigi M, Mancuso C et al (2011) Oxidative and nitrosative modifications of biliverdin reductase-A in the brain of subjects with Alzheimer's disease and amnestic mild cognitive impairment. J Alzheimers Dis 25(4):623–633. https://doi.org/10.3233/JAD-2011-110092
11. Barone E, Di Domenico F, Cenini G, Sultana R, Cini C, Preziosi P, Perluigi M, Mancuso C et al (2011) Biliverdin reductase—a protein levels and activity in the brains of subjects with Alzheimer disease and mild cognitive impairment. Biochim Biophys Acta 1812(4):480–487. https://doi.org/10.1016/j.bbadis.2011.01.005
12. Barone E, Di Domenico F, Cassano T, Arena A, Tramutola A, Lavecchia MA, Coccia R, Butterfield DA et al (2016) Impairment of biliverdin reductase-A promotes brain insulin resistance in Alzheimer disease: a new paradigm. Free Radic Biol Med 91:127–142. https://doi.org/10.1016/j.freeradbiomed.2015.12.012
13. Hanson LR, Frey WH 2nd (2007) Strategies for intranasal delivery of therapeutics for the prevention and treatment of neuroAIDS. J NeuroImmune Pharmacol 2(1):81–86. https://doi.org/10.1007/s11481-006-9039-x
14. Reger MA, Watson GS, Frey WH 2nd, Baker LD, Cholerton B, Keeling ML, Belongia DA, Fishel MA et al (2006) Effects of intranasal insulin on cognition in memory-impaired older adults: modulation by APOE genotype. Neurobiol Aging 27(3):451–458. https://doi.org/10.1016/j.neurobiolaging.2005.03.016
15. Reger MA, Watson GS, Green PS, Wilkinson CW, Baker LD, Cholerton B, Fishel MA, Plymate SR et al (2008) Intranasal insulin improves cognition and modulates beta-amyloid in early AD. Neurology 70(6):440–448. https://doi.org/10.1212/01.WNL.0000265401.62434.36
16. Craft S, Baker LD, Montine TJ, Minoshima S, Watson GS, Claxton A, Arbuckle M, Callaghan M et al (2012) Intranasal insulin therapy for Alzheimer disease and amnestic mild cognitive impairment: a pilot clinical trial. Arch Neurol 69(1):29–38. https://doi.org/10.1001/archneurol.2011.233
17. Apostolatos A, Song S, Acosta S, Peart M, Watson JE, Bickford P, Cooper DR, Patel NA (2012) Insulin promotes neuronal survival via the alternatively spliced protein kinase CdeltaII isoform. J Biol Chem 287(12):9299–9310. https://doi.org/10.1074/jbc.M111.313080
18. Mao YF, Guo Z, Zheng T, Jiang Y, Yan Y, Yin X, Chen Y, Zhang B (2016) Intranasal insulin alleviates cognitive deficits and amyloid pathology in young adult APPswe/PS1dE9 mice. Aging Cell 15(5):893–902. https://doi.org/10.1111/acel.12498
19. Salameh TS, Bullock KM, Hujoel IA, Niehoff ML, Wolden-Hanson T, Kim J, Morley JE, Farr SA et al (2015) Central nervous system delivery of intranasal insulin: mechanisms of uptake and effects on cognition. J Alzheimers Dis 47(3):715–728. https://doi.org/10.3233/JAD-150307
20. Zhang Y, Dai CL, Chen Y, Iqbal K, Liu F, Gong CX (2016) Intranasal insulin prevents anesthesia-induced spatial learning and memory deficit in mice. Sci Rep 6:21186. https://doi.org/10.1038/srep21186
21. Chen Y, Dai CL, Wu Z, Iqbal K, Liu F, Zhang B, Gong CX (2017) Intranasal insulin prevents anesthesia-induced cognitive impairment and chronic neurobehavioral changes. Front Aging Neurosci 9:136. https://doi.org/10.3389/fnagi.2017.00136
22. Nedelcovych MT, Gadiano AJ, Wu Y, Manning AA, Thomas AG, Khuder SS, Yoo SW, Xu J et al (2018) Pharmacokinetics of intranasal versus subcutaneous insulin in the mouse. ACS Chem Neurosci 9:809–816. https://doi.org/10.1021/acschemneuro.7b00434
23. Lochhead JJ, Thorne RG (2012) Intranasal delivery of biologics to the central nervous system. Adv Drug Deliv Rev 64(7):614–628. https://doi.org/10.1016/j.addr.2011.11.002
24. Chauhan MB, Chauhan NB (2015) Brain uptake of neurotherapeutics after intranasal versus intraperitoneal delivery in mice. J Neurol Neurosurg 2 (1)
25. Stanley M, Macauley SL, Holtzman DM (2016) Changes in insulin and insulin signaling in Alzheimer's disease: cause or consequence? J Exp Med 213(8):1375–1385. https://doi.org/10.1084/jem.20160493
26. Oddo S, Caccamo A, Shepherd JD, Murphy MP, Golde TE, Kayed R, Metherate R, Mattson MP et al (2003) Triple-transgenic model of Alzheimer's disease with plaques and tangles: intracellular Abeta and synaptic dysfunction. Neuron 39(3):409–421
27. Cassano T, Romano A, Macheda T, Colangeli R, Cimmino CS, Petrella A, LaFerla FM, Cuomo V et al (2011) Olfactory memory is impaired in a triple transgenic model of Alzheimer disease. Behav Brain Res 224(2):408–412. https://doi.org/10.1016/j.bbr.2011.06.029
28. Cassano T, Serviddio G, Gaetani S, Romano A, Dipasquale P, Cianci S, Bellanti F, Laconca L et al (2012) Glutamatergic alterations and mitochondrial impairment in a murine model of Alzheimer disease. Neurobiol Aging 33(6):1121 e1121–1112. https://doi.org/10.1016/j.neurobiolaging.2011.09.021
29. Bambico FR, Cassano T, Dominguez-Lopez S, Katz N, Walker CD, Piomelli D, Gobbi G (2010) Genetic deletion of fatty acid amide hydrolase alters emotional behavior and serotonergic transmission in the dorsal raphe, prefrontal cortex, and hippocampus. Neuropsychopharmacology 35(10):2083–2100. https://doi.org/10.1038/npp.2010.80
30. Romano A, Pace L, Tempesta B, Lavecchia AM, Macheda T, Bedse G, Petrella A, Cifani C et al (2014) Depressive-like behavior is paired to monoaminergic alteration in a murine model of Alzheimer's disease. Int J Neuropsychopharmacol 18(4):pyu020. https://doi.org/10.1093/ijnp/pyu020
31. Scuderi C, Bronzuoli MR, Facchinetti R, Pace L, Ferraro L, Broad KD, Serviddio G, Bellanti F et al (2018) Ultramicronized

palmitoylethanolamide rescues learning and memory impairments in a triple transgenic mouse model of Alzheimer's disease by exerting anti-inflammatory and neuroprotective effects. Transl Psychiatry 8(1):32. https://doi.org/10.1038/s41398-017-0076-4
32. Giustino A, Cagiano R, Carratu MR, Cassano T, Tattoli M, Cuomo V (1999) Prenatal exposure to low concentrations of carbon monoxide alters habituation and non-spatial working memory in rat offspring. Brain Res 844(1–2):201–205
33. Ripoli C, Piacentini R, Riccardi E, Leone L, Li Puma DD, Bitan G, Grassi C (2013) Effects of different amyloid beta-protein analogues on synaptic function. Neurobiol Aging 34(4):1032–1044. https://doi.org/10.1016/j.neurobiolaging.2012.06.027
34. Ripoli C, Cocco S, Li Puma DD, Piacentini R, Mastrodonato A, Scala F, Puzzo D, D'Ascenzo M et al (2014) Intracellular accumulation of amyloid-beta (Abeta) protein plays a major role in Abeta-induced alterations of glutamatergic synaptic transmission and plasticity. J Neurosci 34(38):12893–12903. https://doi.org/10.1523/JNEUROSCI.1201-14.2014
35. Mayer CM, Belsham DD (2010) Central insulin signaling is attenuated by long-term insulin exposure via insulin receptor substrate-1 serine phosphorylation, proteasomal degradation, and lysosomal insulin receptor degradation. Endocrinology 151(1):75–84. https://doi.org/10.1210/en.2009-0838
36. Miralem T, Lerner-Marmarosh N, Gibbs PE, Tudor C, Hagen FK, Maines MD (2012) The human biliverdin reductase-based peptide fragments and biliverdin regulate protein kinase Cdelta activity: the peptides are inhibitors or substrate for the protein kinase C. J Biol Chem 287(29):24698–24712. https://doi.org/10.1074/jbc.M111.326504
37. Cenini G, Sultana R, Memo M, Butterfield DA (2008) Effects of oxidative and nitrosative stress in brain on p53 proapoptotic protein in amnestic mild cognitive impairment and Alzheimer disease. Free Radic Biol Med 45(1):81–85. https://doi.org/10.1016/j.freeradbiomed.2008.03.015
38. Salim M, Brown-Kipphut BA, Maines MD (2001) Human biliverdin reductase is autophosphorylated, and phosphorylation is required for bilirubin formation. J Biol Chem 276(14):10929–10934. https://doi.org/10.1074/jbc.M010753200
39. Talbot K, Wang HY, Kazi H, Han LY, Bakshi KP, Stucky A, Fuino RL, Kawaguchi KR et al (2012) Demonstrated brain insulin resistance in Alzheimer's disease patients is associated with IGF-1 resistance, IRS-1 dysregulation, and cognitive decline. J Clin Invest 122(4):1316–1338. https://doi.org/10.1172/JCI59903
40. Copps KD, White MF (2012) Regulation of insulin sensitivity by serine/threonine phosphorylation of insulin receptor substrate proteins IRS1 and IRS2. Diabetologia 55(10):2565–2582. https://doi.org/10.1007/s00125-012-2644-8
41. Kapitulnik J, Maines MD (2009) Pleiotropic functions of biliverdin reductase: cellular signaling and generation of cytoprotective and cytotoxic bilirubin. Trends Pharmacol Sci 30(3):129–137. https://doi.org/10.1016/j.tips.2008.12.003
42. Arnold SE, Arvanitakis Z, Macauley-Rambach SL, Koenig AM, Wang HY, Ahima RS, Craft S, Gandy S et al (2018) Brain insulin resistance in type 2 diabetes and Alzheimer disease: concepts and conundrums. Nat Rev Neurol 14:168–181. https://doi.org/10.1038/nrneurol.2017.185
43. King GL, Park K, Li Q (2016) Selective insulin resistance and the development of cardiovascular diseases in diabetes: the 2015 Edwin Bierman Award Lecture. Diabetes 65(6):1462–1471. https://doi.org/10.2337/db16-0152
44. Ge X, Yu Q, Qi W, Shi X, Zhai Q (2008) Chronic insulin treatment causes insulin resistance in 3T3-L1 adipocytes through oxidative stress. Free Radic Res 42(6):582–591. https://doi.org/10.1080/10715760802158448
45. Bell GA, Fadool DA (2017) Awake, long-term intranasal insulin treatment does not affect object memory, odor discrimination, or reversal learning in mice. Physiol Behav 174:104–113. https://doi.org/10.1016/j.physbeh.2017.02.044
46. Adzovic L, Lynn AE, D'Angelo HM, Crockett AM, Kaercher RM, Royer SE, Hopp SC, Wenk GL (2015) Insulin improves memory and reduces chronic neuroinflammation in the hippocampus of young but not aged brains. J Neuroinflammation 12:63. https://doi.org/10.1186/s12974-015-0282-z
47. Lerner-Marmarosh N, Miralem T, Gibbs PE, Maines MD (2007) Regulation of TNF-alpha-activated PKC-zeta signaling by the human biliverdin reductase: identification of activating and inhibitory domains of the reductase. FASEB J 21(14):3949–3962. https://doi.org/10.1096/fj.07-8544com
48. Tundo GR, Sbardella D, Ciaccio C, Grasso G, Gioia M, Coletta A, Polticelli F, Di Pierro D et al (2017) Multiple functions of insulin-degrading enzyme: a metabolic crosslight? Crit Rev Biochem Mol Biol 52(5):554–582. https://doi.org/10.1080/10409238.2017.1337707
49. Association As (2017) Alzheimer's disease facts and figures. Alzheimers Dement 13:325–373
50. Diehl T, Mullins R, Kapogiannis D (2017) Insulin resistance in Alzheimer's disease. Transl Res 183:26–40. https://doi.org/10.1016/j.trsl.2016.12.005
51. Carroll JC, Rosario ER, Kreimer S, Villamagna A, Gentzschein E, Stanczyk FZ, Pike CJ (2010) Sex differences in beta-amyloid accumulation in 3xTg-AD mice: role of neonatal sex steroid hormone exposure. Brain Res 1366:233–245. https://doi.org/10.1016/j.brainres.2010.10.009
52. Hirata-Fukae C, Li HF, Hoe HS, Gray AJ, Minami SS, Hamada K, Niikura T, Hua F et al (2008) Females exhibit more extensive amyloid, but not tau, pathology in an Alzheimer transgenic model. Brain Res 1216:92–103. https://doi.org/10.1016/j.brainres.2008.03.079
53. Oddo S, Caccamo A, Kitazawa M, Tseng BP, LaFerla FM (2003) Amyloid deposition precedes tangle formation in a triple transgenic model of Alzheimer's disease. Neurobiol Aging 24(8):1063–1070
54. Bomfim TR, Forny-Germano L, Sathler LB, Brito-Moreira J, Houzel JC, Decker H, Silverman MA, Kazi H et al (2012) An anti-diabetes agent protects the mouse brain from defective insulin signaling caused by Alzheimer's disease-associated Abeta oligomers. J Clin Invest 122(4):1339–1353. https://doi.org/10.1172/JCI57256
55. Di Domenico F, Barone E, Perluigi M, Butterfield DA (2017) The triangle of death in Alzheimer's disease brain: the aberrant cross-talk among energy metabolism, mammalian target of rapamycin signaling, and protein homeostasis revealed by redox proteomics. Antioxid Redox Signal 26(8):364–387. https://doi.org/10.1089/ars.2016.6759
56. Barone E, Di Domenico F, Mancuso C, Butterfield DA (2014) The Janus face of the heme oxygenase/biliverdin reductase system in Alzheimer disease: it's time for reconciliation. Neurobiol Dis 62:144–159. https://doi.org/10.1016/j.nbd.2013.09.018
57. Tramutola A, Lanzillotta C, Arena A, Barone E, Perluigi M, Di Domenico F (2016) Increased mammalian target of rapamycin signaling contributes to the accumulation of protein oxidative damage in a mouse model of Down's syndrome. Neurodegener Dis 16(1–2):62–68. https://doi.org/10.1159/000441419
58. Di Domenico F, Barone E, Mancuso C, Perluigi M, Cocciolo A, Mecocci P, Butterfield DA, Coccia R (2012) HO-1/BVR-a system analysis in plasma from probable Alzheimer's disease and mild cognitive impairment subjects: a potential biochemical marker for the prediction of the disease. J Alzheimers Dis 32(2):277–289. https://doi.org/10.3233/JAD-2012-121045
59. Selkoe DJ, Bell DS, Podlisny MB, Price DL, Cork LC (1987) Conservation of brain amyloid proteins in aged mammals and humans with Alzheimer's disease. Science 235(4791):873–877

60. Johnstone EM, Chaney MO, Norris FH, Pascual R, Little SP (1991) Conservation of the sequence of the Alzheimer's disease amyloid peptide in dog, polar bear and five other mammals by cross-species polymerase chain reaction analysis. Brain Res Mol Brain Res 10(4): 299–305
61. Triani F, Tramutola A, Di Domenico F, Sharma N, Butterfield DA, Head E, Perluigi M, Barone E (2018) Biliverdin reductase-A impairment links brain insulin resistance with increased Aβ production in an animal model of aging: implications for Alzheimer disease. Biochim Biophys Acta (BBA) Mol Basis Dis doi:https://doi.org/10.1016/j.bbadis.2018.07.005
62. Reger MA, Watson GS, Green PS, Baker LD, Cholerton B, Fishel MA, Plymate SR, Cherrier MM et al (2008) Intranasal insulin administration dose-dependently modulates verbal memory and plasma amyloid-beta in memory-impaired older adults. J Alzheimers Dis 13(3):323–331
63. Benedict C, Hallschmid M, Schmitz K, Schultes B, Ratter F, Fehm HL, Born J, Kern W (2007) Intranasal insulin improves memory in humans: superiority of insulin aspart. Neuropsychopharmacology 32(1):239–243. https://doi.org/10.1038/sj.npp.1301193
64. Chapman CD, Frey WH 2nd, Craft S, Danielyan L, Hallschmid M, Schioth HB, Benedict C (2013) Intranasal treatment of central nervous system dysfunction in humans. Pharm Res 30(10):2475–2484. https://doi.org/10.1007/s11095-012-0915-1
65. Buckner RL, Snyder AZ, Shannon BJ, LaRossa G, Sachs R, Fotenos AF, Sheline YI, Klunk WE et al (2005) Molecular, structural, and functional characterization of Alzheimer's disease: evidence for a relationship between default activity, amyloid, and memory. J Neurosci 25(34):7709–7717. https://doi.org/10.1523/JNEUROSCI.2177-05.2005
66. Vlassenko AG, Vaishnavi SN, Couture L, Sacco D, Shannon BJ, Mach RH, Morris JC, Raichle ME et al (2010) Spatial correlation between brain aerobic glycolysis and amyloid-beta (Abeta) deposition. Proc Natl Acad Sci U S A 107(41):17763–17767. https://doi.org/10.1073/pnas.1010461107
67. Bero AW, Yan P, Roh JH, Cirrito JR, Stewart FR, Raichle ME, Lee JM, Holtzman DM (2011) Neuronal activity regulates the regional vulnerability to amyloid-beta deposition. Nat Neurosci 14(6):750–756. https://doi.org/10.1038/nn.2801
68. Oh H, Madison C, Baker S, Rabinovici G, Jagust W (2016) Dynamic relationships between age, amyloid-beta deposition, and glucose metabolism link to the regional vulnerability to Alzheimer's disease. Brain 139(Pt 8):2275–2289. https://doi.org/10.1093/brain/aww108
69. Willette AA, Modanlo N, Kapogiannis D, Alzheimer's Disease Neuroimaging I (2015) Insulin resistance predicts medial temporal hypermetabolism in mild cognitive impairment conversion to Alzheimer disease. Diabetes 64(6):1933–1940. https://doi.org/10.2337/db14-1507
70. Marks DR, Tucker K, Cavallin MA, Mast TG, Fadool DA (2009) Awake intranasal insulin delivery modifies protein complexes and alters memory, anxiety, and olfactory behaviors. J Neurosci 29(20): 6734–6751. https://doi.org/10.1523/JNEUROSCI.1350-09.2009
71. van der Heide LP, Kamal A, Artola A, Gispen WH, Ramakers GM (2005) Insulin modulates hippocampal activity-dependent synaptic plasticity in a N-methyl-d-aspartate receptor and phosphatidylinositol-3-kinase-dependent manner. J Neurochem 94(4):1158–1166. https://doi.org/10.1111/j.1471-4159.2005.03269.x
72. Chiu SL, Chen CM, Cline HT (2008) Insulin receptor signaling regulates synapse number, dendritic plasticity, and circuit function in vivo. Neuron 58(5):708–719. https://doi.org/10.1016/j.neuron.2008.04.014
73. Lee CC, Huang CC, Hsu KS (2011) Insulin promotes dendritic spine and synapse formation by the PI3K/Akt/mTOR and Rac1 signaling pathways. Neuropharmacology 61(4):867–879. https://doi.org/10.1016/j.neuropharm.2011.06.003
74. Bedse G, Di Domenico F, Serviddio G, Cassano T (2015) Aberrant insulin signaling in Alzheimer's disease: current knowledge. Front Neurosci 9:204. https://doi.org/10.3389/fnins.2015.00204
75. Carlson CJ, White MF, Rondinone CM (2004) Mammalian target of rapamycin regulates IRS-1 serine 307 phosphorylation. Biochem Biophys Res Commun 316(2):533–539. https://doi.org/10.1016/j.bbrc.2004.02.082
76. Perluigi M, Pupo G, Tramutola A, Cini C, Coccia R, Barone E, Head E, Butterfield DA et al (2014) Neuropathological role of PI3K/Akt/mTOR axis in Down syndrome brain. Biochim Biophys Acta 1842(7):1144–1153. https://doi.org/10.1016/j.bbadis.2014.04.007
77. Caccamo A, Majumder S, Richardson A, Strong R, Oddo S (2010) Molecular interplay between mammalian target of rapamycin (mTOR), amyloid-beta, and Tau: effects on cognitive impairments. J Biol Chem 285(17):13107–13120. https://doi.org/10.1074/jbc.M110.100420
78. Caccamo A, Maldonado MA, Majumder S, Medina DX, Holbein W, Magri A, Oddo S (2011) Naturally secreted amyloid-beta increases mammalian target of rapamycin (mTOR) activity via a PRAS40-mediated mechanism. J Biol Chem 286(11):8924–8932. https://doi.org/10.1074/jbc.M110.180638
79. Oddo S (2012) The role of mTOR signaling in Alzheimer disease. Front Biosci (Schol Ed) 4:941–952
80. Bove J, Martinez-Vicente M, Vila M (2011) Fighting neurodegeneration with rapamycin: mechanistic insights. Nat Rev Neurosci 12(8):437–452. https://doi.org/10.1038/nrn3068
81. Gratuze M, Julien J, Petry FR, Morin F, Planel E (2017) Insulin deprivation induces PP2A inhibition and tau hyperphosphorylation in hTau mice, a model of Alzheimer's disease-like tau pathology. Sci Rep 7:46359. https://doi.org/10.1038/srep46359
82. van der Harg JM, Eggels L, Bangel FN, Ruigrok SR, Zwart R, Hoozemans JJM, la Fleur SE, Scheper W (2017) Insulin deficiency results in reversible protein kinase A activation and tau phosphorylation. Neurobiol Dis 103:163–173. https://doi.org/10.1016/j.nbd.2017.04.005
83. Yang Y, Ma D, Wang Y, Jiang T, Hu S, Zhang M, Yu X, Gong CX (2013) Intranasal insulin ameliorates tau hyperphosphorylation in a rat model of type 2 diabetes. J Alzheimers Dis 33(2):329–338. https://doi.org/10.3233/JAD-2012-121294
84. Chen Y, Run X, Liang Z, Zhao Y, Dai CL, Iqbal K, Liu F, Gong CX (2014) Intranasal insulin prevents anesthesia-induced hyperphosphorylation of tau in 3xTg-AD mice. Front Aging Neurosci 6:100. https://doi.org/10.3389/fnagi.2014.00100
85. De Felice FG, Vieira MN, Bomfim TR, Decker H, Velasco PT, Lambert MP, Viola KL, Zhao WQ et al (2009) Protection of synapses against Alzheimer's-linked toxins: insulin signaling prevents the pathogenic binding of Abeta oligomers. Proc Natl Acad Sci U S A 106(6):1971–1976. https://doi.org/10.1073/pnas.0809158106
86. Gispen WH, Biessels GJ (2000) Cognition and synaptic plasticity in diabetes mellitus. Trends Neurosci 23(11):542–549
87. Skeberdis VA, Lan J, Zheng X, Zukin RS, Bennett MV (2001) Insulin promotes rapid delivery of N-methyl-D- aspartate receptors to the cell surface by exocytosis. Proc Natl Acad Sci U S A 98(6): 3561–3566. https://doi.org/10.1073/pnas.051634698